SRESA's International Journal of

LIFE CYCLE RELIABILITY AND SAFETY ENGINEERING

Vol.3 **Issue No.4** **Oct–Dec 2014** **ISSN – 2250 0820**

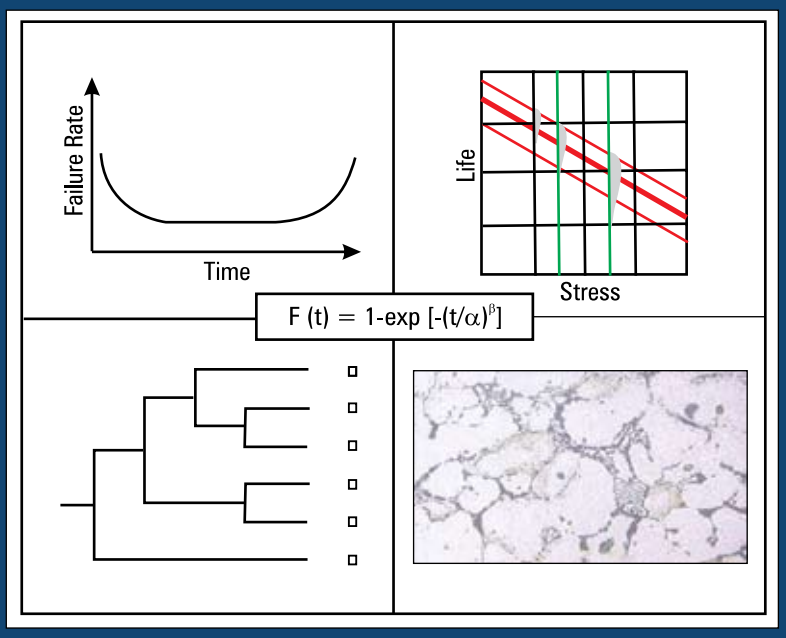

Chief-Editors

P.V. Varde
A.K. Verma
Michael G. Pecht

Society for Reliability and Safety

website: http://www.sresa.org.in

SRESA Journal of Life Cycle Reliability and Safety Engineering

Extensive work is being performed world over on assessment of Reliability and Safety for engineering systems in support of decisions. The increasing number of risk-based / risk-informed applications being developed world over is a testimony to the growth of this field. Here, along with probabilistic methods, deterministic methods including Physics-of-Failure based approach is playing an important role. The International Journal of Life Cycle Reliability and Safety Engineering provides a unique medium for researchers and academicians to contribute articles based on their R&D work, applied work and review work, in the area of Reliability, Safety and related fields. Articles based on technology development will also be published as Technical Notes. Review articles on Books published in the subject area of the journal will also form part of the publication.

Society for Reliability and Safety has been actively working for developing means and methods for improving system reliability. Publications of quarterly News Letters and this journal are some of the areas the society is vigorously pursuing for societal benefits. Manuscript in the subject areas can be communicated to the Chief Editors. Manuscript will be reviewed by the experts in the respective area of the work and comments will be communicated to the corresponding author. The reviewed final manuscript will be published and the author will be communicated the publication details. Instruction for preparing the manuscript has been given on inside page of the end cover page of each issue. The rights of publication rest with the Chief-Editors.

SCOPE OF JOURNAL

System Reliability analysis	**Structural Reliability**	**Risk-based applications**
Statistical tools and methods	Remaining life prediction	Technical specification optimization
Probabilistic Safety Assessment	Reliability based design	Risk-informed approach
Quantitative methods	Physics-of-Failure methods	Risk-based ISI
Human factor modeling	Probabilistic Fracture Mechanics	Risk-based maintenance
Common Cause Failure analysis	Passive system reliability	Risk-monitor
Life testing methods	Precursor event analysis	Prognostics & health management
Software reliability	Bayesian modeling	Severe accident management
Uncertainty modeling	Artificial intelligence in risk and reliability modeling	Risk-based Operator support systems
Dynamic reliability models	Design of Experiments	Role of risk-based approach in Regulatory reviews
Sensitivity analysis	Fuzzy approach in risk analysis	Advanced electronic systems reliability modeling
Decision support systems	Cognitive framework	Risk-informed asset management

SRESA AND ITS OBJECTIVES

a) To promote and develop the science of reliability and safety.

b) To encourage research in the area of reliability and safety engineering technology & allied fields.

c) To hold meetings for presentation and discussion of scientific and technical issues related to safety and reliability.

d) To evolve a unified standard code of practice in safety and reliability engineering for assurance of quality based professional engineering services.

e) To publish journals, books, reports and other information, alone or in collaboration with other organizations, and to disseminate information, knowledge and practice of ensuring quality services in the field of Reliability and Safety.

f) To organize reliability and safety engineering courses and / or services for any kind of energy systems like nuclear and thermal power plants, research reactors, other nuclear and radiation facilities, conventional process and chemical industries.

g) To co-operate with government agencies, educational institutions and research oganisations

SRESA's International Journal of

LIFE CYCLE RELIABILITY AND SAFETY ENGINEERING

Vol.3 Issue No.4 Oct–Dec 2014 ISSN – 2250 0820

SOCIETY FOR RELIABILITY AND SAFETY

Typeset & Printed

EBENEZER PRINTING HOUSE
Unit No. 5 & 11, 2nd Floor, Hind Services Industries,
Veer Savarkar Marg,
Dadar (west), Mumbai -28
Tel.: 2446 2632/ 3872
E-mail: outwork@gmail.com

Life Cycle Reliability and Safety Engineering
Vol.3 Issue 4 (2014) 01-07

Genetic Algorithm Approach based on Markov Model and Basic Path Testing for MIMO Systems in Software testing

R. Sujatha[1], M.Boopathi[1] and C. Senthil Kumar[2]
[1]*Dept. of Mathematics, SSN College of Engineering, Kalavakkam, Chennai, Tamil Nadu, India,*
[2]*Safety Research Institute, Atomic Energy Regulatory Board, Kalpakkam, Tamil Nadu, India*
sujathar@ssn.edu.in

Abstract

In the context of software reliability estimation, Markov Chain model and basic path testing concepts with genetic algorithm (GA) is presented in this paper. An approach to convert control flow graph into a dd-graph is adopted to automatically generate test suites to cover the maximum number of test paths. The weights of the edges of a dd-graph are assigned based on the transition probability matrix. Reliability estimation is done based on the generated test paths. The test - data are converted into a string of binary values which serve as the initial populations. Genetic algorithm is then applied to identify the important path of dd-graph which is the most critical path (mcp) when the component of dd-graph is executed. In this paper a Roulette Wheel type of selection and flipping type of mutation is applied.

Keywords: Genetic Algorithm, Markov Chain, Dd-graph, Basic Path Testing, Transition probability matrix (TPM)

1. Introduction

Software testing is the major part of software development lifecycle. Testing involves finding the test cases and identifying the errors in the program. Generally the aim of software testing is to generate a set of minimal number of test cases such that it reveals as many fault as possible, it can also reduce the cost of the software development. In this paper, concept of basic path testing is used to generate a maximum number of independent paths which are the test cases. Any control flow graph can be modified to a decision to decision graph (dd-graph). We use genetic algorithm optimization technique to identify the most error prone path in a software construct. Genetic algorithm (GA) concept is based on multiple inputs and multiple output method (MIMO). In GA, each individual cover branches of the dd-graph and we are interested to find more important path of dd-graph which is known as the most critical path.

The structure of the paper is in the following way: In section 2 we have discussed the basic concept of Markov chain, genetic algorithm basic concept are explained in section 3, in section 4 software basic path testing concepts are introduced, proposed approach to obtain the most critical path is discussed in section 5, these concepts are illustrated in section 6 and finally concluded.

2. Markov Chain Basic Definitions

In this section the basic concepts of Markov chain are presented in [7].

2.1 Markov Chain

Let $\{X_n\}\ n = 0,1,2,\ldots$ be a sequence of random variables where X_n denotes the state of a system at the n^{th} finite step. If $X_n = j$, then the state of the system at time step n is j, X_0 is the initial state of the system. The Markov property is given by $P(X_n = i_n / X_{n-1} = i_{n-1}, X_{n-2} = i_{n-2}, \ldots, X_0 = = i_0) = P(X_n = i_n / X_{n-1} = i_{n-1})$ i.e., the future state of the system depends only on the present state and, is independent of the past.

Let $P_j(n)$ denote the probability mass function of the random variable X_n, $P_j(n) = P(X_n = j)$ and the conditional probability of the mass function is definedas $P_{ij}(m,n) = P(X_n = j / X_m = i),\ 0 \le m \le n$. The one step transition probability is given by $P_{ij}(1) = P(X_n = j / X_{n-1} = i_{n-1}),\ n \ge 1$ .There are n^2 transition probabilities describing a Markov process can most conveniently be given in the form of an by transition matrix $P = (P_{ij})$.

3. Genetic Algorithm

In this section we present the basic concepts of genetic algorithm [5], [7].

3.1 Genetic algorithm basic concepts

Genetic algorithm is a global optimization technique algorithm inspired by the biological concept of evolution [5], [9]. Genetic algorithm is different from the classical algorithm because for each generation we generate a new set of population, from which an optimal solution is reached. In genetic algorithm, each individual is a member of the population that represents a potential solution to the problem. A chromosome consists of a sequence of genes and the random collection of chromosomes form an initial population. Chromosome can be converted into string of binary values 0 and 1. The algorithm starts, selecting new chromosomes and forms a recombination of new solution and mutation is applied. Then evaluating the fitness value an optimal solution is reached. A pseudo code of genetic algorithm is given below:

Let *P(t)* be the population string at a generation number t,

1. initialize *P(t)*;
2. evaluate *P(t)*;
3. while (stopping condition is not satisfied)
4. do {
5. select *P(t+1)* from *P(t)*;
6. crossover *P(t+1)*;
7. mutate *P(t)*;
8. evaluate *P(t)*;
9. *t=t+1*;
10. }

The above algorithm is iterated until the stopping condition is satisfied. In evaluation step, the fitness of all individuals is evaluated. The evaluation of each chromosome depends on the fitness function.

Selection: Select a set of chromosomes that will be mated to contribute to survive the next generation. Selection of chromosomes depends on its fitness relative to that of other string in the population. In this paper Roultee wheel selection is applied. It is one of the most traditional genetic algorithm selection techniques. The principle of Roulette wheel selection is a linear search through a Roulette wheel with the slots in the wheel weighted in proportion to the fitness values. Each individual is assigned a slice of the Roulette wheel, the size of the slice being proportional to the individual's fitness and if slice of the wheel is very small, the occurrence for the next cycle is very poor. The particular chromosome cannot appear for the next generation.

Crossover: The crossover is an important operator in a genetic algorithm. The crossover operates between any two chromosomes in a population which are randomly selected. The swapping of genes between chromosomes to produce a better offspring that is, new chromosome will have a good genetic material from old chromosome and survive to the next generation with crossover probability p_c. When crossover does not happen the new chromosomes are immediately copied from the parents.

Mutation: After crossover, mutation is performed bit-by-bit basis. The mutation is applied on a randomly selected single chromosome by making bitwise change. The genes are flipped (0 and 1 are interchanged) with mutation probability p_m. Suppose mutation is not performed the resulting chromosomes after crossover are directly copied from parents. In this paper flipping type of mutation is applied.

4. Concepts of Basic Path testing and Dd-graph

A case study of control flow graph (CFG) is directly assumed [8]. Any node in a dd-graph [1, 2, 4] does not have only one entering arc and one existing arc. Nodes denote either decision or junction or condition i.e. forking of the control flow and merging of the control flow. Program block are directly connected to the arcs, in this way, the size of the dd-graph is shrunk, and the control flow is immediately captured. Hence the modified CFG is known as dd-graph and it is denoted by G_{ddg}.

4.1 Dd-graph

A dd-graph is a graph *G=(V,E)* where *V* is the set of nodes (vertices) and *E* is the set of arcs (edges), with two different arcs e_1, e_k. Where e_1 is the unique entry arc and e_k is the unique exit arc, and any other arc in *E* is reached by e_1 and reaches e_k. For any $n \in N$, $n \neq Tail(e_1)$, $n \neq Head(e_k)$, *(indegree (n) + outdegree (n))>2,* while *indegree (Tail* (e_1)*)=0* and *outdegree (Tail* (e_1)*) = 1, indegree (Head* (e_k)*) = 1* and *outdegree (Head* (e_k)*)=0.*

4.2 Algorithm for basic path testing

Tom Mc-Cabe first introduced basis path testing approach [1, 4]. The basis path method is a white box testing technique and helps the test case designers to derive a logical complexity measure of a procedural design and use this measure as a guide for defining a basis set of execution paths. Test cases derive to exercise the basis set are guaranteed to execute every statement in the program at least one time during testing.

The logical complexity of the program can be estimated by using cyclomatic complexity. In the case of basis path testing, cyclomatic complexity defines the number of independent path in the basis set of a program and provides an upper bound for the number of test that must be conducted to ensure that all statements is to be executed at least once. An independent path is any path through program that includes at least a new processing statement or a new condition. When stated in terms of a flow graph, an independent path move along at least one edge that has not been traversed before the path is defined. Cyclomatic complexity in graph theory and provides us with extremely useful software metric. Cyclomatic complexity for a graph G is defined as $V(G)=E-N+2$, where E is the number of edges of a dd – graph, N is the number of nodes in a dd – graph. Let $V(G)=P+1$, where $P$is the number of predicate nodes in a dd – graph.

4.3 Algorithm for finding the mcp of dd-graph and its reliability

Input: Chromosome type (n, m)

Output: The best chromosome and its fitness value when the component is executed also calculate system reliability.

1. Begin
2. Change the control flow graph into dd-graph
3. Initialization: Assigning the weights of a dd-graph based on TPM. Write the (TPM) matrix
4. Apply basic path testing to compute the maximum number of independent component by $V(G) = E - N + 2$. Let T_i be the path corresponding to test cases
5. Choose the input values for dd-graph program based on the path
6. Apply genetic algorithm
7. Calculate the next generation based on the formula in section V-A. Iterate, Identifying the most critical path
8. Compute the system reliability using the expression presented in section V - B
9. End

5. Proposed Approach

In this section we present the proposed approach to calculate fitness value of dd-graph.

5.1 Assigning weights

The test data generation is performed using genetic algorithm and a fitness function is computed. The technique uses a weighted dd-graph based path testing to search the program domain for suitable test cases that cover every possible path in the software under test. However, it is not always possible to cover all probable paths:

(i) The code may contain an infinite number of paths, if dd-graph has loops,

(ii) The number of paths in a program is exponential to the total number of branches in it and many of them may be unfeasible.

(iii) The number of test cases becomes very large, since each path can be covered by several test cases.

Therefore, the problem of path testing selects a subset of paths to execute and find test data to cover it.

For any dd-graph the algorithm assigns weights to the edges of dd-graph. One method used to estimate the relative frequencies of traversal of different edges and vertices is to assume the program digraph, in which the weight p_{ij} of edge (n_i, n_j) is the conditional probability that the program execution will go to program block n_j given that it has executed program block n_i. Once the program reaches n_k, the stop vertex, the probability of its, branching to any other vertex is zero. We add a self loop of weight one at vertex n_k. Thus n_k is the absorbing state, the only absorbing state in the system, and remaining vertices correspond to the transient states. At each node of dd-graph the incoming credit is divided and distributed to all outgoing edges of the node. For any node having only one outgoing edge, the incoming weight is assigned to the particular edge [6].

A method for optimizing software testing efficiency is done by identifying most critical path in a dd-graph. Using basic path testing we generate a maximum number of independent paths which are the test cases. A dd-graph can be split in to finite number of branches. Assume that the numbers of branches being tested in a dd-graph are taken in column and numbers of individuals are taken in a row. A visible type of population fitness function is required, since all the branches of a program are to be completely tested for each individual [2].

Suppose there are n branches in a dd-graph and m individuals in a population. There are mn items being tested, a branch coverage matrix B is given by:

$$B = \begin{matrix} 1 \\ 2 \\ \vdots \\ m \end{matrix}\begin{bmatrix} f_{11} & f_{12} & \cdots & f_{1n} \\ f_{21} & f_{22} & \cdots & f_{2n} \\ \vdots & \vdots & \ddots & \vdots \\ f_{m1} & f_{m2} & \cdots & f_{mn} \end{bmatrix} \quad (1)$$

The matrix values are estimated by assigning the weights when the individual i passes through branch j and f_{ij} is calculated. Otherwise zero.

Calculate next generation using the following procedure:

(i) For each individuals i, we have $F_i = \sum_{j=1}^{m} f_{ij}$. Where F_i is the fitness value of each individuals.

(ii) Compute the probability of selection of chromosome for next generation, the percentage of fitness is given by $P_i = \frac{F_i}{\sum_{j=1}^{m} F_i}$ and sum of all P_i is one (j=1,2,…,m) can be obtained and fitness percentage probability value is calculated.

(iii) Expected count is given by

$$\text{Expected count} = \frac{\text{Individual fitness}}{\text{Average fitness}}$$

where. $\text{Average fitness} = \frac{\text{Sum of all fitness}}{\text{Total number of individuals}}$

The expected count gives an idea to find the (mating pool) actual count to decide how many better chromosomes survive to the next generation. Hence the total actual count gives the number of chromosome that survives in each generation.

5.2 Reliability Evaluation of the system

Let $T_i, i = 1, 2, \cdots, n$ be the independent paths and R_i be the reliability of paths T_i The value of R_i is calculated using tpm of the underlying dd-graph. The system reliability R_s can be expressed as

$$R_s = P\left(\bigcup_{i=1}^{n} T_i\right)$$

$$= \sum_{i=1}^{n} P(T_i) - \sum_{i=1}^{n}\sum_{j>i}^{n} P(T_i \cap T_j) + \sum_{i=1}^{n}\sum_{j>i}^{n}\sum_{k>j}^{n} P(T_i \cap T_j \cap T_k) + \ldots + (-1)^{n-1} P(T_1 \cap \cdots \cap T_n)$$

$$= \sum_{i=1}^{n}\prod_{l \in T_i} R_l - \sum_{i=1}^{n}\sum_{j>i}^{n}\prod_{l \in T_i \cup T_j} R_l + \sum_{i=1}^{n}\sum_{j>i}^{n}\sum_{k>j}^{n}\prod_{l \in T_i \cup T_j \cup T_k} R_l + \cdots + (-1)^{n-1}\prod_{l \in \bigcup_{i=1}^{n} T_i} R_l$$

6. Illustration

The program code and its dd-graph is given below [8]:

```
0.  gcd(int n, int m)  {
    int r;
1.  if(n > m)  {
    r = m;
    m = n;
    n = r; }
2.  r = m%n;
3.  while(r != 0) {
    m = n;
    n = r;
    r = m%n; }
    return n; }
```

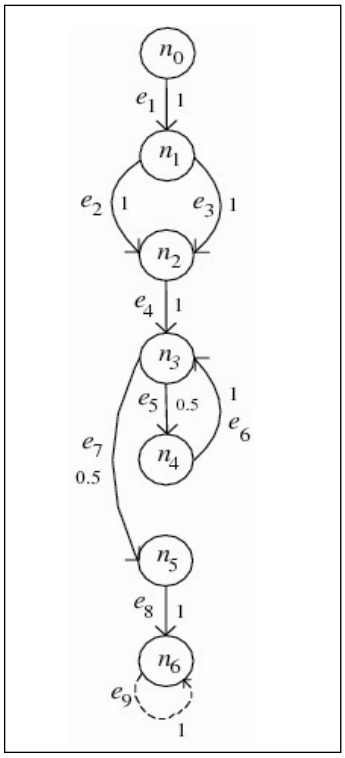

Fig.1. Program dd-graph of Markov chain and its weights

Figure 1 shows the nodes are represented by n_0 to n_6 , where the starting node is n_0 and final node is n_6. The edges are denoted by e_1 to e_8. The beginning edge is e_1 and final edge is e_8. The program line code of the parts of dd-graph and weights are assigned as shown in Table 1. The weights are assigned in the basis of stochastic matrix form.

The transition probability of the Markov chain is given by:

$$B = \begin{matrix} n_0 \\ n_1 \\ n_2 \\ n_3 \\ n_4 \\ n_5 \\ n_6 \end{matrix}\begin{bmatrix} 0 & 1 & 0 & 0 & 0 & 0 & 0 \\ 0 & 0 & 1 & 0 & 0 & 0 & 0 \\ 0 & 0 & 0 & 1 & 0 & 0 & 0 \\ 0 & 0 & 0 & 0 & 0.5 & 0.5 & 0 \\ 0 & 0 & 0 & 1 & 0 & 0 & 0 \\ 0 & 0 & 0 & 0 & 0 & 0 & 1 \\ 0 & 0 & 0 & 0 & 0 & 0 & 1 \end{bmatrix} \quad (3)$$

Table 1 Program line code and its components of dd-graph

S. No.	1	2	3	4	5	6	7	8	9	10	11	12	13	14	15
Line Code	0	0-1	1	1-2	2	2-3	3	3-4	4	4-3	3-5	5	5-6	6	6 - 6
Components	n_0	e_1	n_1	e_2/e_3	n_2	e_4	n_3	e_5	n_4	e_6	e_7	n_5	e_8	n_6	e_9
Weights	–	1	–	1	–	1	–	0.5	–	1	0.5	–	1	–	1

Based on the basic path testing concepts, the maximum number of test path is obtained by the formula *E-V+2* where *E* is the number of edges and *V* is the number of vertices. In this example we have 9 edges and 7 vertices and the number of predicate node is 2. Hence *8-7+2=3*. Therefore *V(G) =2+1* which is the maximum number of test path is obtained.

To apply genetic algorithm we consider the possible four test cases which are independent paths, given by

$$\begin{aligned} T_1 &= 0-1-2-3-5-6, \\ T_2 &= 0-1-2-3-5-6, \\ T_3 &= 0-1-2-3-4-3-4-3-5-6, \\ T_4 &= 0-1-2-3-4-3 \end{aligned} \tag{4}$$

The initial chromosomes are selected for the above paths which traces the path of the program line code. Figure 2. shows the branch coverage representation of the dd-graph is given below:

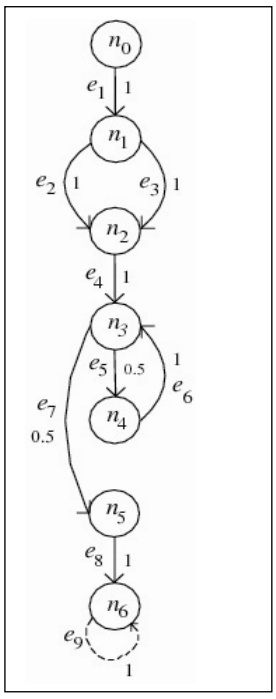

Fig.2. Branch coverage matrix representation of dd-graph

There 4 test paths are generated from the initial population (randomly selected) and dd-graph can be split into 7 branches. Here A , B , C , D , E , F , G are the branches and the initial population (n, m) are (12, 4), (4, 8), (15, 4) , (7, 12).

The Branch coverage matrix, B is given by

$$B = \begin{array}{c} \\ (12,4) \\ (4,8) \\ (15,4) \\ (7,12) \end{array} \begin{array}{c} \begin{array}{ccccccc} A & B & C & D & E & F & G \end{array} \\ \begin{bmatrix} 1 & 1 & 0 & 1 & 0 & 0.5 & 1 \\ 1 & 0 & 1 & 1 & 0 & 0.5 & 1 \\ 1 & 1 & 0 & 1 & 3 & 0.5 & 1 \\ 1 & 0 & 1 & 1 & 4.5 & 0.5 & 1 \end{bmatrix} \end{array} \tag{5}$$

In this part, using the test cases we apply genetic algorithm, to find a most critical path. The first generation test cases that form an initial population are randomly selected and converted into binary type of chromosomes [3]. Fitness value and its percentage of fitness value, expected value, actual count are computed using the formula presented in section 4. In Table. 2 calculations corresponding to the first generation are given. The test case (7, 12) travels the path $0-1-2-3-4-3-4-3-4-3-5-6$ and fitness value is 9.0. This directly be calculated from the branch coverage matrix by adding the entries of F_4 The actual count decides the number of best chromosomes which survive for the next generation. The expected count of a chromosome is low it cannot survive to next generation. Because the next Roultee wheel, the same chromosome have low expected probability count.

In Table. 3, mutation and crossover are carried out to the chromosomes that survived from the first generation. Single point crossover and flipping type of mutation is applied to generate a new set of chromosomes thus getting second generation. For the second generation the fitness value, actual count calculations are carried out and the process is continued to get better chromosomes. The best chromosome and its fitness value are shown in Table 6, which helps in the identification of the most critical path.

Table 2 Selections of Chromosomes (Generation-1)

S. No	Chromosome (n, m)	Binary string	F(x) value	Probability fitness	Fitness percentage	Expected count	Actual count
1	(12, 4)	1100 0100	4.5	0.1764	17.64	0.7059	0
2	(4, 8)	0100 1000	4.5	0.1764	17.64	0.7059	0
3	(15, 4)	1111 0100	7.5	0.2942	29.42	1.1765	2
4	(7, 12)	0111 1100	9.0	0.3530	35.30	1.4117	2
Sum	–	–	25.5	1.0000	100.00	4.0000	4
Avg	–	–	6.375	0.2000	20.00	1.0000	1
mcp	(7, 12)	0111 1100	9.0	0.3530	35.30	1.4117	2

Table 3 Crossover and mutation (Generation-2)

S. No.	String no.	Mating pool	After crossover	Mutation flipping	Mutation chromosome
1	3	(15, 4) 1111 0100	(15, 12) 1111 1100	0000 0111	(15, 11) 1111 1011
2	3	(15, 4) 1111 0100	(15, 12) 1111 1100	0001 0010	(14, 14) 1110 1110
3	4	(7, 12) 0111 1100	(7, 4) 0111 0100	0100 0000	(3, 4) 0011 0100
4	4	(7, 12) 0111 1100	(7, 12) 0111 1100	1111 0111	(8, 11) 1000 1011

Table 4 Selection of Chromosomes

S. No.	Chromosome (n, m)	Binary string	F(x) value	Probability fitness	Fitness percentage	Expected count	Actual count
1	(15, 11)	1111 1011	8.0	0.2910	29.10	1.1637	2
2	(14, 14)	1110 1110	4.5	0.1637	16.37	0.6546	0
3	(3, 4)	0011 0100	6.0	0.2181	21.81	0.8727	0
4	(8, 11)	1000 1011	9.0	0.3272	32.72	1.3090	2
Sum	–	–	27.5	1.0000	100.00	4.0000	4
Avg	–	–	6.875	0.2500	25.00	1.0000	1
mcp	(8, 11)	1000 1011	9.0	0.3272	32.72	1.3090	2

Table 5 Crossover and Mutation (Generation -3)

S.No.	String no.	Mating pool	After crossover	Mutation flipping	Mutation chromosome
1	1	(15, 11) 1111 1011	(15, 4) 1111 0100	0000 1111	(15, 11) 1111 1011
2	1	(15, 11) 1111 1011	(15, 11) 1111 1011	0010 0110	(13, 13) 1101 1101
3	4	(8, 11) 1000 1011	(8, 4) 1000 0100	0000 1111	(8, 11) 1000 1011
4	4	(8, 11) 1000 1011	(8, 11) 1000 1011	0010 0000	(10, 11) 1010 1011

Table 6 Selection of Chromosomes

S.No	Chromosome (n, m)	Binary string	F(x) value	Probability fitness	Fitness percentage	Expected count	Actual count
1	(15, 11)	1111 1011	8.0	0.2909	29.09	1.1636	2
2	(13, 13)	1101 1101	4.5	0.1636	16.36	0.6546	0
3	(8, 11)	1000 1011	9.0	0.3273	32.73	1.3091	2
4	(10, 11)	1010 1011	6.0	0.2182	21.82	0.8727	0
Sum	–	–	27.5	1.0000	100.00	4.0000	4
Avg	–	–	6.875	0.2500	25.00	1.0000	1
mcp	(8, 11)	1000 1011	9.0	0.3273	32.73	1.3091	2

The reliability values of T_1, T_2, T_3, T_4 are 0.5, 0.5, 0.125, 0.0625 respectively. Calculate the system reliability using the formula presented in section V-B. The system reliability is 0.794921875.

7. Conclusion

In this paper we have used the concept of Markov Chain and software basics path testing to form a maximum number of independent paths as an initial population for application of genetic algorithm, instead of choosing an arbitrary initial population. The basic path testing ensures total branch coverage. However, construction of basic path testing depends on the size of the program.

Acknowledgement

The authors thank Atomic Energy Regulatory Board India (Project No. AERB/CSRP/Project No: 53/06/2013) for providing financial assistance to carry out this work. The authors thank SSN management for support and Co-Investigator Dr. S. Narasimman.

References

1. Chinnaiyan R., Somasundram S., "Reliability Estimation Model for Software Components Using CEP", International Journal of Mechanical and Industrial Engineering, Vol 2, No. 2, pp. 89 - 93, 2012.
2. Dan Liu., Xuejun wang., and Jianmin wang., "Automated Test Data generation Based On genetic algorithm", Journal of Theoretical and Applied Information Technology, Vol 48, No. 1, pp. 411-416, 2013.
3. Harmen - Hinrich Sthamer., "The Automatic Generation of Software Test Data Using Genetic Algorithms", Ph.D., Thesis, University of Glamorgan, 1995.
4. Debasis Mohapatra., "GA based Test Case Generaton Approach for Formation of Efficient Set of Dynamic Slices", International Journal on Computer Science and Engineering, Vol 3, No. 9, pp. 3265 - 3274, September 2012.
5. Mitchell Melanie., An Introduction to Genetic Algorithms, First MIT Press paperback edition, Fifth printing, 1999.
6. Narsingh Deo, Graph Theory with Applications to Engineering and Computer Science, Prentice – Hall of India, 2002.
7. Kishore S Trivedi,, "Probability & Statistics with Reliability, Queuing and Computer Science Applications", John Wiley & Sons, Inc, Second Edition, 2008.
8. Praveen Ranjan Srivastava., Tai-hoon Kin., "Application of Genetic Algorithm in Software Testing", International Journal of Software Engineering and its Application, Vol 3, No. 4, pp. 87-95, 2009.
9. Sivanandam S.N., Deepa S.N., "Introduction to Genetic Agorithm", Springer, 2008.

Life Cycle Reliability and Safety Engineering
Vol.3 Issue 4 (2014) 08-12

Latent Manufacturing Flaws Cause Parametric Degradation

R.Muthukumar, D.Damodaran
Centre for Reliability, STQC Directorate, V.S.I.Estate, Thiruvanmiyur, Chennai-600041, India
muthukumar@stqc.nic.in

Abstract

Electronic device parametric degradation is often due to latent and incipient flaws created out of the manufacturing process. Inter-metallic formation, moisture absorption, die attach problems are some of the latent flaws which can cause real life device performance issues in the field. The flaws remain subtle all through the fabrication process, but upon subjecting the devices to repeated thermal and electrical stresses in the field, the anomalies surface to result in detectible failures. These defect sites in the semiconductor devices become voltage-trapping sites leading to hot spot generation. This can lead to high current drawn through the bond wires, forward voltage drops and intermittent gain degradation. The expansion of the moisture vapour, unwanted gas occupying the voids in the die attach medium and the different co-efficient of expansion of dissimilar material combinations in the inter-metallic, result in ground loss problems also. These defects lead to poor electrical performance of these devices. This paper presents three case studies made on such failing devices along with the results of the failure analysis done on these devices. The results of the analysis can be helpful in overcoming the type of defects attributable to device manufacturing process thus improving the device Reliability to a greater extent.

Keywords: latent flaws, incipient flaws, micro-cracks, die attach, hot spot

1. Introduction

Manufacturing process defects of electronic components are an increasing area of concern. These defects often lie latent within the device all through the fabrication process [1]. They even pass through the quality inspection and testing phase of the production line. Finally they manifest in the field due to continuous operation under field stress conditions. Some of these defects are high moisture absorption of green chips during wafer growth, inter-diffusion of n and p type materials resulting in dissimilar material combinations forming inter-metallic in the junction area, inter-metallic in the aluminium – silicon bonding or gold silicon bonding, purple plagues, micro crevices or voids in the die attach medium etc. These subtle defects at the device level, remains dormant all through the fabrication process, but manifests in the field in the form of degraded performance in electrical characteristics, output gain, ground loss etc. An attempt is made in this paper to discuss these subtle failures and their effects in high-reliability applications. Three case studies are discussed here to address these types of defects. Analysis was carried out by comparing two good devices and 4 defective devices in each case. In all these three cases a tailored thermal cycling proved to be an effective screen to grow the defective sites into a full grown failure thus helping us to weed out such defects in the field. A typical screen is given at the end, which can be used to stimulate such latent defects during the production screening activity.

2. Case of Moisture Absorption

Some of the transistor amplifiers used in Inverters, failed in parametric degradation mode were taken up for failure cause determination. D.C. characteristics were measured on the defective devices and the failure mode confirmed to be high emitter to base forward voltage. The apparent reason can be high voltage drops across the wafer or the anomalies in the bond pad area. As per the published design specifications, the base to emitter saturation voltage is around 420mV and the forward emitter to base voltage shall be in the order of 1.35V to 1.85 Volts. The good and failed devices were checked for these parameters. It was observed that the forward base to emitter voltage (V_{FBE}) was more than the tolerance limits in the defective units, in the order of 2.29V and the base to emitter saturation voltage ($V_{BE\,sat}$) also was on the higher side, in the order of 534 to 712mV. Correspondingly there was lot of variation

in collector to emitter voltage (V_{CE}) in the order of 39.3mV to 71.7mV.

Table 1 Results – Electrical Characteristics

Parameters / Devices	Units	$V_{BE\ Sat}$ (mV)	V_{FBE} (V)	V_{CE} (mV)	I_{CB} (nA)
Good	1	420	1.35	26.5	8.98
	2	419	1.85	27.3	9.02
Defective	1	534	2.29	39.3	9.12
	2	622	2.34	46.7	12.12
	3	683	2.75	59.4	15.73
	4	712	2.86	71.7	17.25

Therefore the collector to base current also fluctuated between 9.12nA to 17.25nA. It could be seen that there was cumulative effect on the device electrical performance. The results of the electrical measurements taken in two good devices and four defective devices are presented in the Table I above.

These failed devices were moulded with phenolic compounds for convenience of handling during sample preparation for sectioning. Selectively the moulds were grinded and polished using coarse and fine grades of grinding papers. Finally the die was sectioned. It is observed at a certain stage that there is complete out gassing of the moisture absorbed by the chip during processing of the device. The devices have high mobility of electrons with low forward voltage drop. The forward current expected is in the order of 379mA. But some of these devices exhibited high forward voltage drop across the device thus reducing the mobility of electrons resulting in drop in forward current. Because of the out gassing of the trapped moisture in the porous substrate, micro crevice was formed in the die. Due to this thinning of the conductive path has taken place and hence the current flow is restricted. This lead to voltage drop across the conductive paths and leads to electrical characteristic degradation of the devices. The crevice formed is occupied by unwanted moisture vapour and upon accumulation of heat in the application, this vaporous band of moisture expands and contracts to the disadvantage of the good device performance. Further the current flow paths will be narrowed down to the conductive area only and hence the anomaly becomes voltage-trapping sites resulting in high voltage drops. This is the reason for the resultant high forward emitter to base voltage. Such entrapped moisture can be cooked off by airing the chip to the curing temperature and long exposure during fabrication. The problem can be attributed to manufacturer process related problem and it is a latent flaw. Controlling of such devices from getting into the active circuit can be done through thermal cycling screen, which is much effective in bringing out such defects [5]. If allowed to get into the field they exhibit high instability in electrical properties and cause irretrievable loss to the system performance.

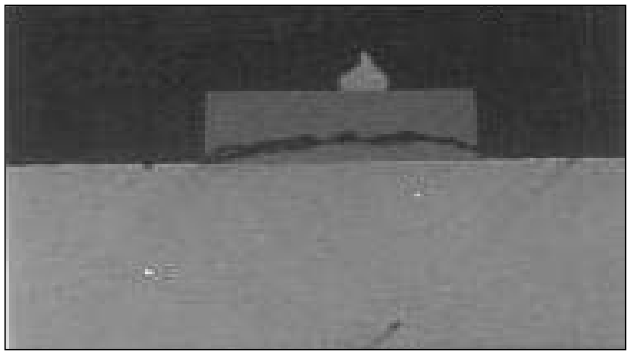

Fig. 1 View of Micro crevice formed in the wafer due to entrapped moisture

In the field due to repeated operations the voltage trapping sites accumulate heat generating a hot spot. If hot spot persists high current flows through this hot spot resulting in high current drawn through the bond wires. This one time may exceed the melting point of wire and the semiconductor itself, resulting in metal run through the crevice, resulting in short circuit. This will lead to the metallisation of the die directly shorting with the header with the metal run through the epoxy die-attach to the header. The basic problem of moisture absorption is manufacturer related and hence by selection of proper materials and proper process curing methods this can be minimized. A detailed incoming screening program will weed out such defective devices from surfacing at a later stage in the field after getting into the customers hands thus improving the device Reliability [2].

3. Case of Inter-metallic Formation

A group of high Power transistors, reported to have failed in high collector to emitter voltage and reduced collector current failure mode were taken up for root cause analysis. It is found that the collector – emitter junction characteristics varied widely from a forward collector to emitter voltage (V_{FCE}) of 1.32V to 2.45V with collector to emitter current (I_{CE}) ranging from 0.39 Amps to 0.51Amps. Collector to emitter breakdown voltage (V_{CEb}) has increased from 47V to 76V. These devices are used in inverters as power transistors. High current gain is demanded at the output as these devices are operating at high load conditions in the field. In some of the devices collector to emitter direct shorting was also seen. The failure

mode was confirmed through electrical parameter verification. The results of the electrical measurements taken in two good devices and four defective devices are presented in the Table II below.

Table 2 Results – Electrical Characteristics

Parameters / Devices	Units	$V_{FCE\ Sat}$ (V)	V_{CEb} (V)	I_{CB} (A)
Good	1	0.87	47	0.29
	2	0.93	48	0.36
Defective	1	1.32	68	0.39
	2	1.87	72	0.43
	3	2.42	73	0.48
	4	2.45	76	0.51

These devices were sectioned with standard molding compounds followed by selective grinding and polishing exercise. It was observed that the devices had inter-metallic formation at the die attach area resulting in gold growing into copper and vice-versa. The inter-metallic is due to improper contact formation between the Gold loaded epoxy over the header with the semiconductor wafer. Further there was a band of inter-metallic seen in the die attach area due to inter-diffusion of Gold and Copper plating over it. The inter-metallic formation can take longer time in the field. However once the process is initiated the anomaly has a telling effect on the ground current flow ultimately disturbing the electrical performance of the devices. These defects may remain subtle throughout the manufacturing process to finally fail in the field. The collector and emitter contact integrity is lost due to these incipient defects in the bonding and die-attach area [3]. Especially the drops in collector current (Ic) with increase in collector to emitter voltage (VCE) caused by hot spot phenomena because of raised emitter temperature are due to inter-metallic formation between different materials of the devices. If the primary bonding metal is Gold then there is great variation in the electrical properties of the devices. Greater parts of Gold make a highly non reactive and good contact. The visibility of any one of the plagues will drive us to the conclusion that there are other plagues present as well. When examined, it was observed that the devices had inter-metallic formation at the emitter bonding area resulting in white plagues or purple plagues. Also bond wire lifting is seen. Micro cracks around the tail end of the bond wires are also seen. The inter-metallic is due to improper contact formation between the Gold bond wire and the aluminium metallisation. These plagues cause serious bond and die attach failures.

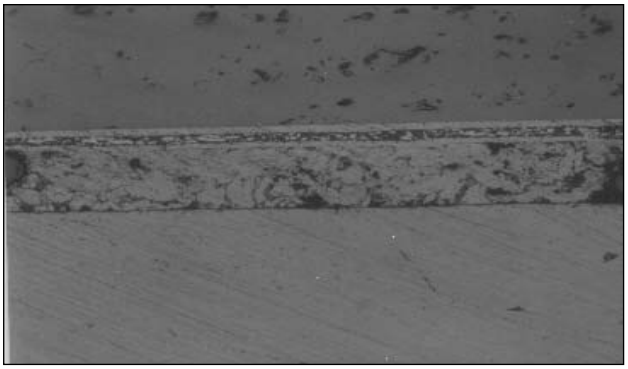

Fig. 2 Inter-metallic formation in the die attach area in a high power transistor

The failure mode observed during parametric measurements in the failed devices indicates that they are time dependent failures [6]. Under continued operation in the field for longer duration these defects surface. Thermal Cycling at a very high rate of change of temperature in the order of 20°C/min. when adopted as a production process screen would bring out these defects to enhance the device Reliability [4].

4. Case of void Formation in the Die Attach

A group of transistors used in frequency converters, Driver Amplifiers etc., failed in the field in the output gain reduction mode were reported for root cause analysis. The device specification is that output Power is 12 dBm @ 6.5GHz. The Collector to Emitter Voltage (V_{CE}) is in the order of 2.5V Min. and 3.6V Max. The V_{CE} Vs I_C curves for the devices fluctuated between two V_{CE} values. The fluctuation of collector current (I_C) was from I_C 64mA @ V_{CE} 3.4V and Ic 49mA @ V_{CE} 4.1V. The gain decreased in some of the devices from 14.04 dBm to 8.90 dBm intermittently and the devices recover after momentary freaks. Intermittency is given in the following figure.

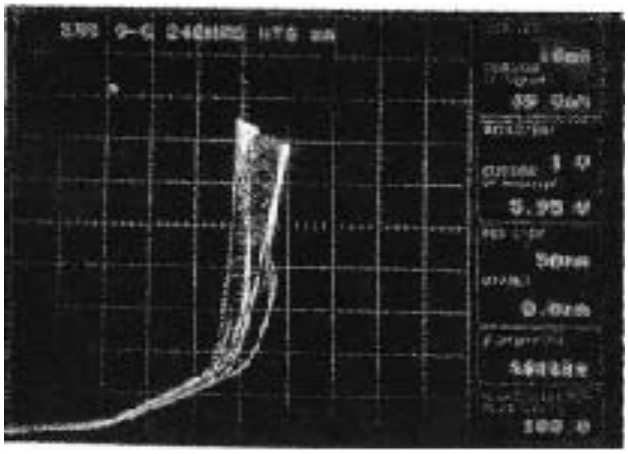

Fig. 3 Intermittency in electrical characteristics between output and ground.

There was a corresponding drop in collector current associated with output voltage increase. In some devices permanent failure such as the gain reduction was seen.

Table 3 : Results – Electrical Characteristics

Parameters / Devices	Units	Power @ 65 GHz (dBM)	V_{CE} (V)	I_C (mA)
Good	1	13.8	3.4	64
	2	14.0	3.3	65
Defective	1	8.9	4.93	49
	2	9.2	4.98	49
	3	9.1	5.01	48
	4	9.4	5.04	50

The devices were of SMT technology and of miniature size. Therefore for easy handling, and as an ESD protection, transoptic materials were used for moulding them safely. Surface view of some of the devices revealed that there is no metallization or gross defects noticed in the die. The devices were sample prepared and grinded / polished on a step-by-step process to finally detect the problems of the die, the bond wires, the bonding area, the die attach medium or the header area.

It is observed that voids are present in the die attach medium, the Silver loaded epoxy which serves as a good electrical and thermal conducting medium. The ground is supplied to the devices through this path. In some devices the voids were so big that there was no path for ground currents to flow. As such ground is totally lost to the device and the resulting gain reduction. The voids have occurred because of out gassing or complete burn out of the organic content in the die attach medium because of excessive heat operation in the field. Further it is noticed that the epoxy settles down away from the active circuitry. This has lead to voids formation in the long run. The voids could also develop because of air or gas entrapment during epoxy application during fabrication process or due to evaporation of organic content during curing. The intermittency in gain could be due to limiting of the ground current flow through only the areas of continuous conducting path, except the void areas. In reality some current may flow through the semiconductor leading to the decrease in output current, because of the high electrical resistivity of the semiconductor. Consequently temperature rise and voltage rise will be moderate and intermittent until a very large void is formed. The gases in the voids expand and contract during operation and create micro cracks in the surrounding metallization and the bonding area. This results in fluctuating field performance. These defects are subtle defects, which have been produced out of device manufacturing process. A well-designed Thermal Cycling Screen can eliminate these defects and make the devices to stabilize in their parameters [9]. However if it is a pattern type of failure the root cause is to be identified and the screening parameters shall be accordingly tightened to prevent such anomalies from being reported from the field.

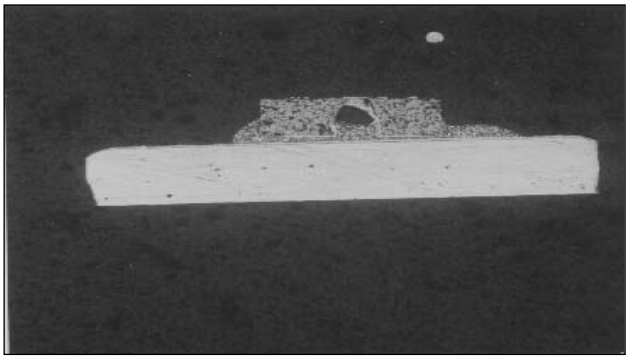

Fig. 4. Void formation due to epoxy content settling away from the active circuitry

The above failure modes observed in the above devices need some accumulation of thermal and electrical stress over a period of time. Then only the inherent weakness in the die will be surfaced. Hence the thermal cycling screen has to be designed properly. An adequate screen has to be dynamic as the factors influencing the anomalies keep varying and the device technology would have attained higher maturity. Accordingly the screen parameters have to be tightened [10]. Elimination of screen can be there only after the confidence on the Reliability performance of the device has improved multifold.

5. Thermal Cycling Screen

The thermal cycling has been arrived at based on experimentation by adopting the step-by-step process [7] of incrementally advancing the stress from the operating limit. The failure criteria for the units for continuous monitoring of the health of the units were fixed as fluctuation in I_C, V_{CE}, Power, V_{BE}, load current etc. The first step was from -20°C to +70°C. This progressed up to -55 °C to +100°C while all the defective units were detected in the first two case studies given above. The number of cycles in each case was 20 with 10 under energized condition and another 10 without energizing. However in the third case the screening was conducted for 50 cycles of temperature

cycling under energized condition. The device needed huge accumulation of heat to give out its weakness. A typical thermal cycling screen specification arrived at for the above devices is given in the table below.

Table 4: Thermal Cycling Screen

Factors	Specification Range
Temperature Range	-55°C to +100°C
Dwell Time	15 minutes
Rate of Change of temperature	At least 20°C/min.
Air Velocity within the Chamber	1.8 meters/sec
Number of cycles	(20) 10 + 10
Conditioning	Energized for 10 cycles and Un-energized for 10 cycles

The units were subjected to Thermal Cycling as stimulator and Electrical parametric Verification as detector [8] of the failure mechanisms alternately.

6. Conclusion

The failure modes observed in the above devices have been related to the manufacturing process anomalies. For these defects to surface there is need for accumulation of thermal and electrical stress for a long period of time. Occurrence of such failures in the field leads to loss of customer good will and eventually losing the market share. A careful design of the thermal cycling screen as a production screening mechanism can detect these failures early. Thus the latent manufacturing flaws causing parametric degradation in electronic devices can be effectively addressed.

References

1. Ireson, W.G.Coombs, C.F. & Moss R. "Handbook of Reliability Engineering and Management", Mcgraw Hill, 1996, New York, USA.
2. Peter W.Becker, and Finn Jensen, "Design of Systems and Circuits for maximum Reliability or Maximum Production Yield", McGraw Hill, 1997, USA, 24 – 30.
3. Hu, J.M., Pecht, M., and Dasgupta, A., "Design of Reliable Die attach in Microelectronics Packaging," International Journal of Microcircuits and Electronic packaging, Vol 16, No. 1, pp. 1-21, 1993.
4. Pecht, M., Lall, P., and Whelan, S.J. , "Temperature dependence on Microelectronic Device Failures", Quality and Reliability Engineering International, Vol. 6, pp. 275-284, 1990, 6:275 – 284.
5. O' Coonor, P.D.T. "Practical Reliability Engineering", John Wiley and Sons, New York, 1996.
6. Handbook of Accelerated Life testing methods – technical paper, RADC-TR-67-420, W.Yurkowsky 1967.
7. The institute of environmental science and Technology (IEST), p52-54, USA, July-Aug 1996.
8. Harry W. McLean, HALT, HASS & HASA Explained: 31 – 53, 2000.
9. Caruso, H. , "Significant subtleties in Stress Screening", Proceedings of the Institute of Environmental Sciences (IEST), 1983 154 – 158.
10. Wong, K. "A new environmental stress screening theory for electronics", 1989.

Life Cycle Reliability and Safety Engineering
Vol.3 Issue 4 (2014) 13-23

Numerical Finite Element Investigation on Laser Cladding of Aerospace Components

Ramesh Raju[1], Vijay Petley[2], Arun G. K.[1], Muthukannan Duraiselvam[1], Shweta Verma[2], Rajendran R.[2]
[1]*Department of Production Engineering, National Institute of Technology, Tiruchirappalli, Tamil Nadu, India,*
[2]*Gas Turbine Research Establishment, Defense Research & Development Organization, Bangalore, India*
mrramesh2002@gmail.com

Abstract

A three dimensional finite element coupled thermo-mechanical model is used to simulate the laser cladding of Nickel super alloy powder on nickel super alloy substrate using three dimensional conical Gaussian heat source. Effect of laser beam power and scanning speed on dilution, heat affected zone, and residual stresses are analyzed and the process is optimized. This parametric study makes use of the simulation algorithm programmed as a macro routine within the ANSYS 14.5 using ANSYS Parametric Design Language. The adaptability of finite element model is verified experimentally and they are found to be in good agreement with each other.

Keywords: Laser cladding; thermo-mechanical model; finite element simulation; dilution; residual stress

1 Introduction

Laser cladding is a method of depositing material by which a powdered or wire feedstock material is melted and consolidated by use of a laser in order to coat part of a substrate or fabricate a near-net shape part. It can also be used to improve the hardness, wear resistance and to change the mechanical and metallurgical properties. The main advantage of laser-cladding process is the possibility of obtaining high quality material deposition on complex parts like aero engine blades which have undergone service induced degradation. Thus laser cladding can be applied in the repair of high value and safety critical parts. This ability is especially useful for high cost parts that present wears or local damage due to severe operating conditions. Different types of parts can be processed, such as housings, blades or even complete turbine rotors. Once the parts are repaired by laser cladding, they can be reassembled which reduces lead times and manufacturing cost.

Turbine blades are the most critical parts of an aero engine, faced to harsh environments and long-hours of running at high temperature and pressure which may promote service induced degradation. The degradation may have a metallurgical or mechanical origin and deteriorate the creep, fatigue, impact and tribological properties. Defects like distortion, wear, impact dents and cracks are formed due to these reasons which can be fatal and the financial costs would be high. In order to circumvent these problems, repair and overhaul is an inevitable choice to extend the service life of the blade as the replacement is far more expensive due to the continual increase in raw material and manufacturing cost. Laser cladding is a promising technique for turbine blade refurbishment which is capable of depositing material on complex part with minimum distortion.

The most critical and challenging aspect of blade refurbishment is to build defect free layer with uniform mechanical and metallurgical properties which should be similar to the bulk properties of the wrought blade. The uniqueness of the worn components and its complex repair requirements demands an adaptive laser cladding with close control of parameters. The laser cladding technique allows the deposition of an alloy or coating material on a metal or metal alloy, achieving an excellent metallurgical bond between both materials. In addition it will generate a smaller heat affected zone (HAZ) and lower distortions. Also narrow interface zone (intermixing zone) and reduced susceptibility to cracking. Complex relationships exist among the process parameters and the simultaneous thermo-mechanical phenomena which generally occur during the laser beam interaction with the clad and the substrate materials. The finite element (FE) method can furnish important preliminary information about the thermal and mechanical stresses induced by thermal cycles.

The analyses of both the temperature and the stress distributions in the laser cladding process were performed through a 3D thermo-mechanical finite element model to analyze the laser cladding treatment using powder blown on a ring part by Palumbo et al. [2]. Lei et al. made a three dimensional model to simulate high power laser clad coatings on Ti6Al4V alloys. The temperature distribution, three dimensional shape and size of TiC melting region, molten pool and heat affected zone (HAZ) of the substrate were obtained using this FE model [3]. To obtain a uniform thickness of a thin walled blade, the temperature field distribution was calculated by the numerical simulation by Zhu et al.[4]. The thin walled blade's curvature change and accumulating layer number was studied and the effect of accumulating layer number on temperature field distribution and effect of curvature change on temperature distribution was investigated in this study. Hao et al. built a 3D thermal FE model for the simulation of temperature field in the laser cladding of Ti6Al4V alloy [5]. Instead of directly acquiring the geometric parameters of cladding layer and heat source for a concrete FE simulation through the measured data in experiments, this model is able to achieve temperature distributions for laser cladding with varying combinations of process parameters by constructing an adaptive cladding layer and moving heat source model using an inverse modeling approach. It is found that to have potential to be applied in the thermal simulation of laser cladding with varying process parameters, considering the variation of the characteristic dimensions of deposition bead and the heat source. Tseng et al.[6] proposes a tailored laser heat source model for the finite element analysis of the laser cladding process. In his work he developed a tailored laser heat source model that comprehensively takes the physical characteristics and focusing conditions of the laser beam in to consideration. This heat source model was then integrated in a finite element laser cladding model to simulate laser cladding using the pre-placed powder layer technique. Hofmana et al. suggests a model which uses a novel approach to determine the clad geometry[7]. The correlation between observable melt pool characteristics and dilution is investigated using this model. Simulations were performed for different combinations of cladding speed, laser power (distribution) and substrate temperature. Due to the high thermal gradients produced by the laser processes and the mismatch in the material properties, significant stresses could develop inside the material, sometimes leading to unacceptable distortions on the piece or the appearance of cracks. Because of the complexity of the process and the large number of parameters involved, a numerical model will help to get a better understanding of it. The stresses generated in the laser cladding technique result from the high thermal gradients involved. They could lead to undesirable distortions or even crack formation, therefore the prediction of the temperatures, strains and stresses during the process results in its better understanding, besides, it could allow some optimization. A transient nonlinear thermo-mechanical FEM model [8] was developed for this task by Suárez et al. The heat input to the developed model by Siva Shanmugam is assumed to be a three dimensional conical Gaussian heat source[9]. However, the effect of laser parameters such as beam power, speed and energy density for multilayer cladding process to optimize the process have not been studied much in detail by the researchers for laser cladding. In this Study a three dimensional (3D) finite element (FE) coupled thermo-mechanical model is used to simulate the laser cladding of Nickel super alloy powder on nickel super alloy substrate using 3D conical Gaussian heat source. Effect of laser beam power and scanning speed on dilution, HAZ, and residual stresses are analyzed and the process is optimized. This parametric study makes use of the simulation algorithm programmed as a macro routine within the ANSYS 14.5 using ANSYS Parametric Design Language (APDL). The adaptability of FE model is verified experimentally and then it is investigated that for a fixed energy density.

2. Theoretical Aspects

2.1 Thermal analysis

When a volume is bounded by an arbitrary surface, the balance relation of the heat flow is expressed by:

$$-\left(\frac{\partial R_x}{\partial x}+\frac{\partial R_y}{\partial y}+\frac{\partial R_z}{\partial z}\right)+Q(x,y,z,t)=\rho C\frac{\partial T(x,y,z)}{\partial x} \quad (1)$$

where Rx, Ry and Rz are the rates of heat flow per unit area, T(x,y,z) is the current temperature, Q(x,y,z) is the rate of internal heat generation, ρ is the density, C is the specific heat and t is the time. The model can then be completed by introducing the Fourier heat flow as:

$$Rx = -kx\frac{\partial T}{\partial x} \quad (2a)$$

$$Ry = -ky\frac{\partial T}{\partial y} \quad (2b)$$

$$Rz = -kz\frac{\partial T}{\partial z} \quad (2c)$$

where kx, ky and kz are the thermal conductivities in the x, y and z directions, respectively. Generally, the material parameters kx, ky, kz, ρ and C are temperature dependent. Inserting Eqs. (2a), (2b) and (2c) into Eq. (1) yields:

$$\left(\frac{\partial}{\partial x}\left(kx\frac{\partial T}{\partial x}\right)+\frac{\partial}{\partial y}\left(ky\frac{\partial T}{\partial y}\right)+\frac{\partial}{\partial z}\left(kz\frac{\partial T}{\partial z}\right)\right)+Q=\rho C\frac{\partial T}{\partial t} \quad (3)$$

The general solution is obtained by applying the following initial and boundary conditions:

$$T(x,y,z,0) = T0(x,y,z) \quad (4)$$

The heat transfer per unit area (QA) due to convection is expressed as:

$$QA = h(T-T\alpha) \quad (5)$$

where h is the convection heat transfer coefficient and Tα is the surrounding temperature. Film coefficient is considered as independent upon temperature. Heat transfer due to radiation is not considered in this model because it not a variable and will not have significant effect in the model. Solving Eq. (3) by considering the boundary conditions expressed in Eqs. (4) and (5) gives the temperature distribution in the body. This temperature field will then be applied in the mechanical model to calculate the residual stresses.

The temperature fields and the evolution of the residual stresses are investigated by using finite element method. In order to accurately capture the temperature fields and the residual stresses in the weld, a 3-D finite element model is developed. The heat conduction problem is solved independently from the stress problem to obtain temperature history. However, the formulation considers the contributions of the transient temperature field to the stress analysis through the thermal expansion, as well as temperature dependent thermo-physical properties. The material properties are assumed to be temperature dependent. All analyses are performed using the finite element analysis software ANSYS 14.5 using APDL.

2.2 Mechanical analysis

The equilibrium and constitutive equations used here to conduct elastic–plastic mechanical analysis are described below:

Equations of equilibrium:

$$\sigma ij,j + \rho bi = 0 \quad (6)$$

here, σij is the stress tensor and bi is the body force. It is assumed that the stress tensor is symmetrical, i.e. $\rho_{ij} = \rho_{ji}$

Elastic–plastic constitutive equations:

$$[D\sigma] = Dep\ [d\epsilon] - [Cth]dT \quad (7a)$$

$$[Dep] = [De]+[Dp] \quad (7b)$$

where [De] is the elastic stiffness matrix, [Dp] is the plastic stiffness matrix, [Cth] is the thermal stiffness matrix, dσ is the stress increment, dϵ is the strain increment and dT is the temperature increment. Since thermal elastic–plastic analysis is a non-linear problem, the incremental calculation technique is employed here in solving the problem. The incremental stress can be obtained by using the full Newton–Raphson method.

3. Finite Element Modelling

3.1 Modelling of laser cladding process

Two FE models were developed: the first one for the uncoupled heat transfer analysis (to get the temperature distribution); the second one for the stress analysis (assigning as input the previously calculated temperature field).ANSYS Finite Element Modelling commands can be translated to create a log file with commands to model, load, solve and analyze the laser cladding. Multi pass laser cladding of a Nickel based alloy powder on a same alloy substrate was analyzed using a finite element model. The substrate have dimensions of 30mm (L) ×2mm (W) ×12 mm (H), as shown in Fig. 1. The model was meshed in to 23040 elements and 26901 nodes.The powder layer on the substrate surface had dimensions of 30 (L) × 2mm (W) × 1.25mm (T) as shown in fig. 2 .The desired width of 2mm is based on the thickness of the substrate given in the FE model. For modeling the clad deposition process, the whole clad track was divided into slices of 0.5 mm thickness. In practice, the substrate was

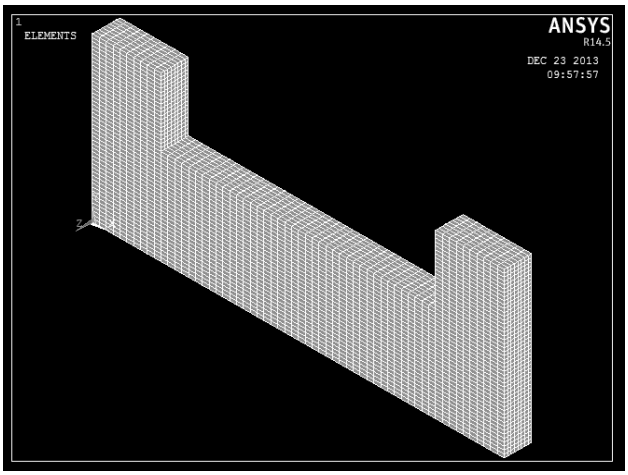

Fig. 1 Finite element mesh model of substrate

fixed on the workbench, so the substrate model was constrained in the x-direction.

Heat conduction within the work piece model, and free convection between the surfaces of the work piece and the surrounding air are considered in the modeling. A parametric approach was adopted to define the mesh density in the substrate; in particular it was related to the laser spot diameter.

The mesh is finer in the substrate and clad because of the strong temperature gradients originated during the process. Solid 185 a thermal 3D brick element, which has a 3D thermal conduction capability, is utilized to mesh the entire FEM. Also, it is defined by eight nodes having three degrees of freedom at each node. In addition, in order to depict the process of mass transfer due to powder deposition on substrate, the element birth and death technique is applied to the 3D thermal analysis.

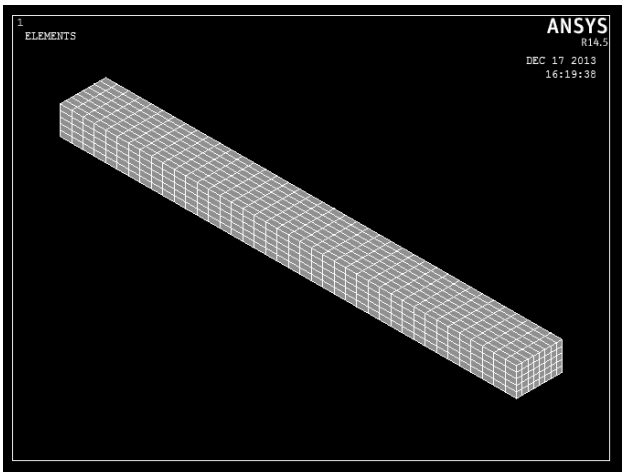

Fig. 2 Finite element mesh model of clad layer

3.2 Heat source model

In this work, a three-dimensional conical Gaussian heat source (volumetric heat source) is used as a laser source and it is applied to specific elements in the finite element model. In this the power density deposited region is maximum at the top surface of work piece, and is minimum at the bottom surface of work piece. Along the work piece thickness, the diameter of the power density distribution region is linearly decreased. However, the heat density at the central axis is kept constant. The expression for 3D conical Gaussian heat source used in the analysis is given in Eq. (8).

$$Q_v(r,z) = \frac{2P}{\pi r_0^2 H} e^{1-\left(r/r_0\right)^2} \left(1 - \frac{z}{H}\right) \quad (8)$$

Where Qv is the laser power intensity, r0 is the laser spot radius, H is the sheet thickness, r is the current radius, i.e. the distance from the cone axis, and z is the vertical axis.

The temperature dependent material properties of material are shown in Fig. 3, such as conductivity, modulus of elasticity and coefficient of linear expansion are applied to the model.

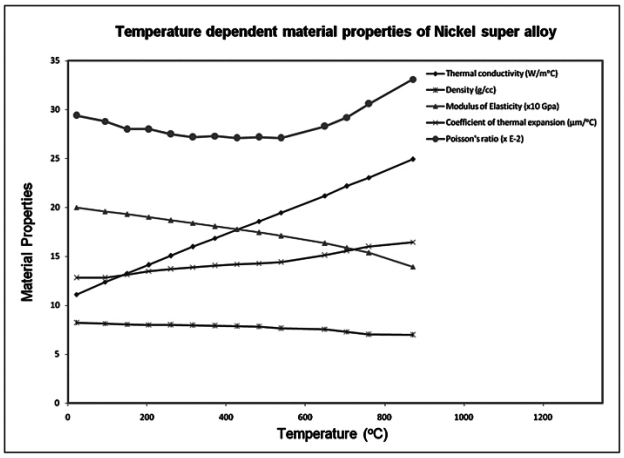

Fig. 3 Temperature dependent material properties of Ni based super alloy

3.3 Laser Cladding Parameters for Simulation

Table 1 Laser Cladding Parameters

Laser power	1500 W
Laser spot diameter	2 mm
Powder feed rate	8 gm/min

For simulation of laser cladding initially four different combinations of parameters are considered.

Table 2 Initial set of parameters for simulation

Sl no	Power (W)	Processing speed (mm/min)	Time taken for depositing(s)
1	1500	400	3
2	1500	500	2.4
3	1500	600	2
4	1500	750	1.6

3.4 Assumptions and boundary conditions

The following points are taken into account while developing the finite element model:

- Natural convection of 15W/m2K is applied over the entire surface of specimens except at the region where heat flux is applied.

- To consider the boundary conditions, associated with convection, on the surface of the work piece, a reference temperature of 200C is applied.
- A small amount of heat is lost by radiation from the surface layer. So influence of heat loss due to radiation is neglected in the analysis.
- Phase transformations are not considered.
- Several factors can reduce the net absorbed laser energy: partial reflection on the deposited metal, absorption by in-flight powder and absorption by evaporating metal from the pool. In this work laser energy transfer efficiency was assumed as 30%.
- Thermal properties of the material such as conductivity, specific heat, density are temperature dependent.
- Latent heat of fusion and vaporization are not considered in this model.

4. Finite Element analysis

4.1 Thermal analysis

The thermal model is aimed at simulating the complex thermal interactions occurring at the clad–substrate interface. The clad powders absorb energy directly from the laser beam and indirectly from the work piece: the substrate uses only a part of the laser energy to melt and to heat the surrounding material, while reflects the remaining energy to the clad. In the FE simulation the clad elements were progressively activated assigning them the Nickel base super alloy thermal conductivity, specific heat, coefficient of linear expansion, elastic modulus and density values.

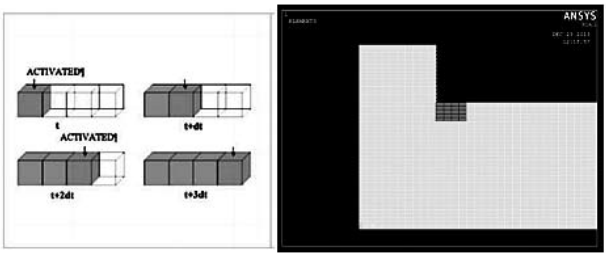

Fig. 4 Schematic illustration of the progressive activation of clad elements

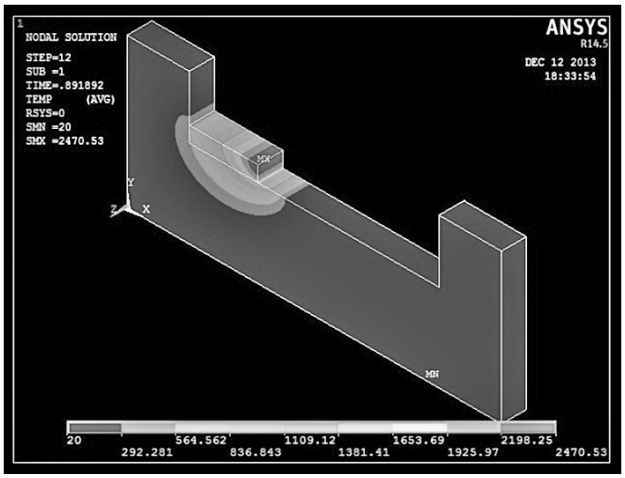

Fig. 5 (a) Temperature distribution during laser cladding at initial clad

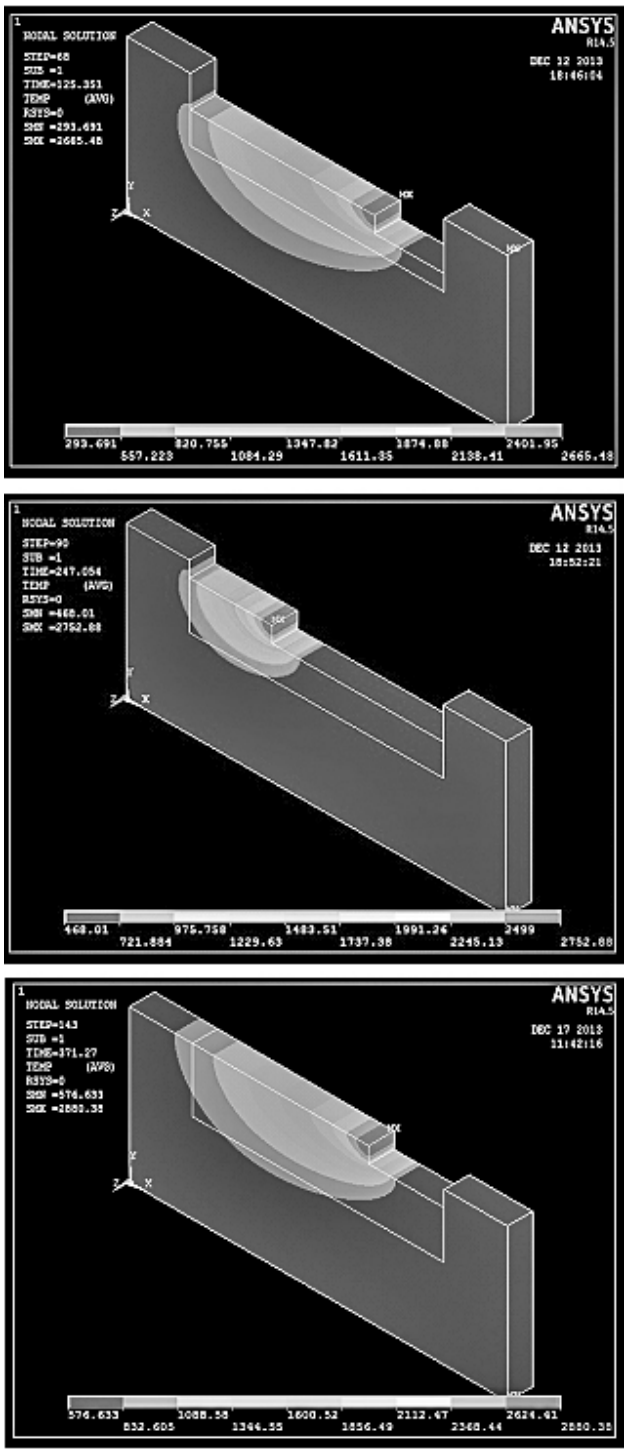

Fig. 5(b) Temperature distribution during laser cladding at various time steps

The values of these temperature dependent physical properties are input by using ANSYS Parametric Design Language (APDL) available in finite-element code, ANSYS. The heat transfer model was thus able to simulate: the thermo-physical characteristics of the substrate and the clad material, the convection boundary conditions with the air and the heat conduction at the clad–substrate interface by means of general temperature-dependent conductivity.

The clad layer elements were present in the model from the beginning of the analysis. The powder gradual deposition on the substrate was simulated defining a first step in which the clad element set was removed from the model. In the following steps, the position of the laser beam was varied and, at the same times, a fixed number of clad elements were activated as illustrated in Fig. 4. In each step the clad elements were activated by specifying their thermo-physical properties; only clad elements/nodes which lied inside the laser spot were activated using APDL. Thermal loads were assigned to the activated clad elements from the centre of the laser Gaussian energy distribution. Towards the end of each layer a cooling step of 120 sec was defined to simulate the heat flux dissipated by the clad layer through air and the surrounding material at room temperature. Fig. 5(a) and 5(b) are showing the temperature distribution during laser cladding at various time steps.

4.2 Mechanical analysis

In the model the thermal and the mechanical fields are sequentially coupled. Therefore, the temperature field inside the material during all the process is computed first with a transient thermal analysis, and then these results are given as a thermal load to the mechanical analysis. The Fig. 6 is showing the equivalent stress in the clad layer predicted by the 3D model. The quasi-static mechanical analysis has the previous results as the thermal load and constraints only in the two-end face as compared to the holding of the work piece during the cladding. More complicated material models could represent the mechanical behavior near the melted zone more accurately, but the lack of material data, especially at high temperatures is the major drawback.

5. Results and Discussions

5.1 Thermal cycles across the clad layer and substrate

Fig. 7 illustrates the thermal cycles during the deposition of first clad layer with 1500W power and processing speed of 400mm/min. It considered a predefined node path located in the longitudinal axial symmetric section across the clad layer and the adjacent substrate region. Time taken for deposition of one layer is 3 sec. All the clad nodes (Nc) and three nodes in the substrate (Ns) reach the melting temperature of the material (1260°C).This indicates that melting will happen to a depth of 0.75 mm in the substrate. Only some of the nodes in the clad reach a maximum value of about 2560°C that is lower than the clad boiling point (2917°C). The nodes of the clad mesh rapidly reach the melting point after their activation, while the temperature peak for the substrate nodes is delayed; No difference between the clad and the substrate behavior exists in the cooling phase. The mesh nodes which reach the high temperature achieve high cooling rates.

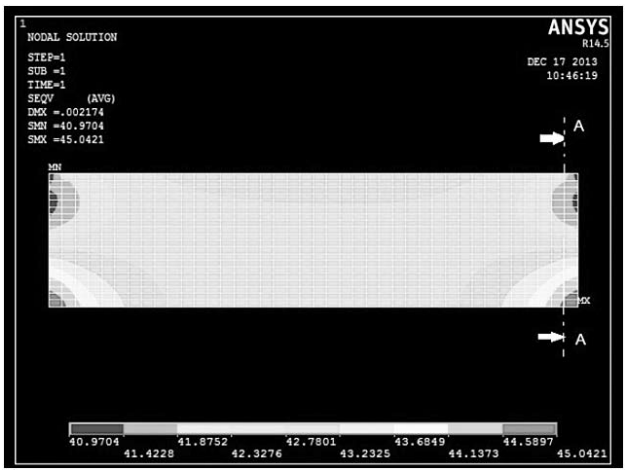

Fig. 6 Equivalent stress in the clad layer predicted by the 3D model

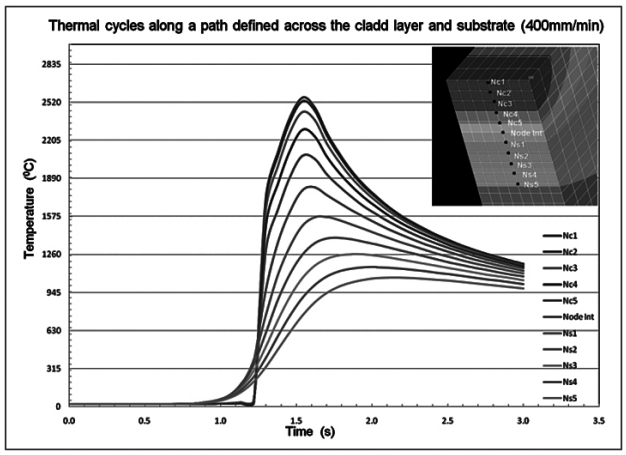

Fig. 7 Thermal cycles across clad and substrate for speed 400mm/min

Fig. 8 illustrates the thermal cycles for 1500W power and processing speed of 500mm/min. It highlights that, time taken for deposition of one layer

is 2.4 sec. All the clad nodes (Nc) and one nodes in the substrate (Ns) reach the melting temperature of the material (1260°C). This indicates that melting will happen to a depth more than 0.25 mm in the substrate. Only some of the nodes in the clad reach a maximum value of about 2225°C that is lower than the clad boiling point. Fig.9 illustrates the thermal cycles for 1500Wpower and processing speed of 600mm/ min highlights that, the time taken for deposition of one layer is 2 sec. All the clad nodes (Nc) and node at clad substrate interface (Node Int.) reach the melting temperature of the material (1260°C). This indicates that melting will happen to a depth less than 0.25 mm in the substrate. Only some of the nodes in the clad reach a maximum value of about 1968°C that is lower than the clad boiling point. Fig. 10 illustrates the thermal cycles for 1500W power and processing speed of 750mm/min highlights that, time taken for deposition of one layer is 1.6 sec. All the clad nodes (Nc) reach the melting temperature of the material (1260°C). But with this speed it is failed to provide the heating necessary to melt clad substrate interface. Cladding may not be possible. Only some of the nodes in the clad reach a maximum value of about 1682°C that is lower than the clad boiling point.

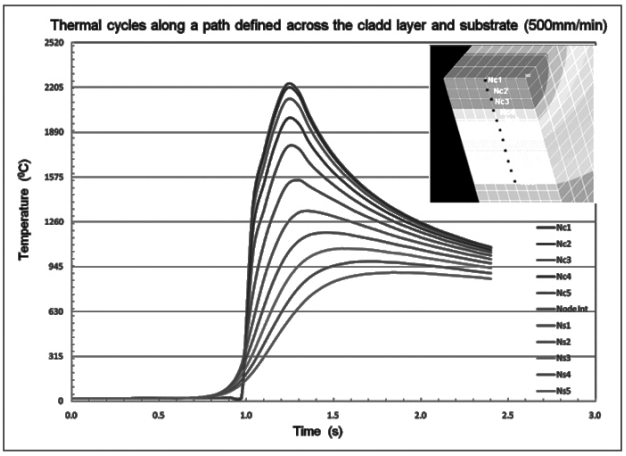

Fig. 8 Thermal cycles across clad and substrate for speed 500mm/min

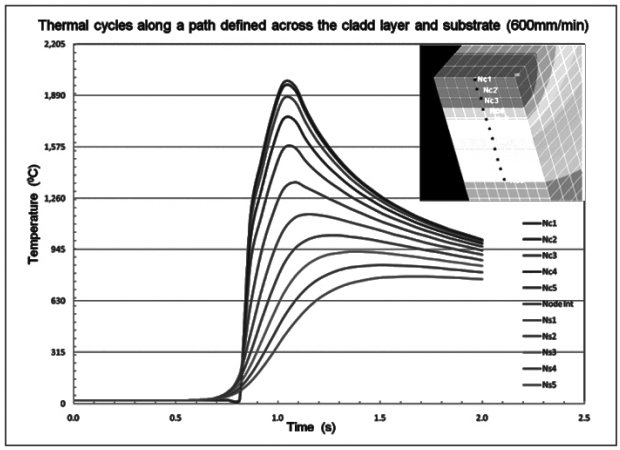

Fig. 9 Thermal cycles across clad and substrate for speed 600mm/min

5.2 Effect of process parameters on dilution

An important quality aspect of the clad layer is the dilution of the deposited clad layer material, i.e. the extent of mixing between the clad material and the base material. Even though a certain minimum mixing is necessary to guarantee a good bonding, an excessive mixing is not desirable. The maximum dilution was limited in the range of 15- 30% [2]. Fig. 11 shows a schematic of transverse cross section of the clad track.

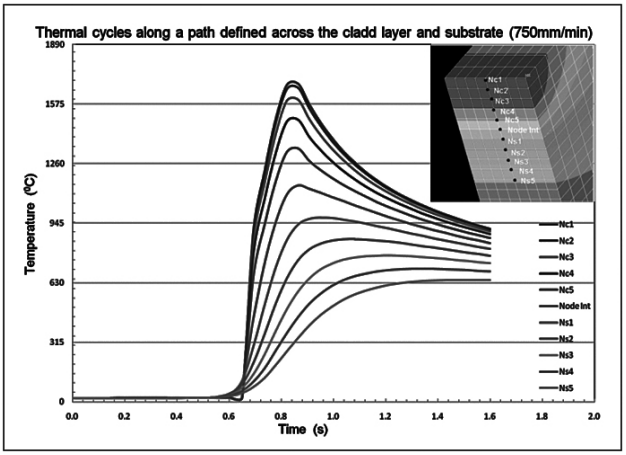

Fig. 10 Thermal cycles across clad and substrate for speed 750mm/min

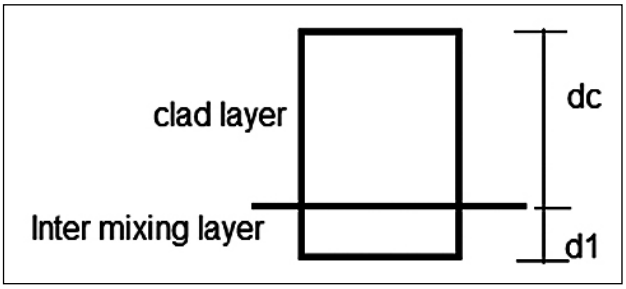

Fig. 11 Schematic representation of transverse cross section of the clad track

It is possible to define the dilution D = d1 / (d1+dc) × 100. Based on simulation a plot is made between temperature and depth of dilution (Fig. 12). Table 3 represents the dilution (D) for various parameters.

From the dilution values it is clear that cladding with 1500W power and speed of 500mm/min is showing satisfactory result.

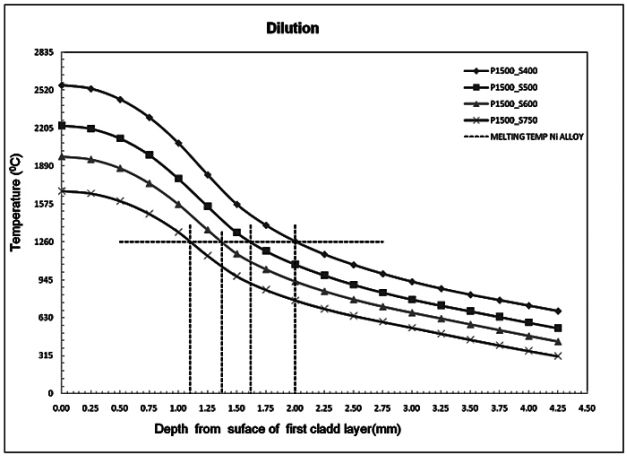

Fig. 12 Variation in depth of dilution with different parameters

5.3 Effect of process parameters on heat affected zone

Isothermal boundary at allotropic transformation temperature of nickel based super alloy (720°C) is used to characterize HAZ of the substrate is shown in Fig. 13 represents the shape of HAZ of the substrate, it appears as semi-ellipsoid shape. To get more details about the HAZ in laser cladding the temperature distribution on the path (as shown in Fig. 13) was investigated. The variation dimensions of the HAZ with different parameters are shown in the Fig. 14 and the values are noted in the table 4.

Table 3 Dilution values for different parameters

Parameter	d_1	$d_{1+}d_c$	D
P 1500 S 400	0.75	2	37.5%
P 1500 S 500	0.37	1.62	22.8%
P 1500 S 600	0.125	1.375	9%
P 1500 S 750	-	-	Less than 1%

P=Power, S=Speed

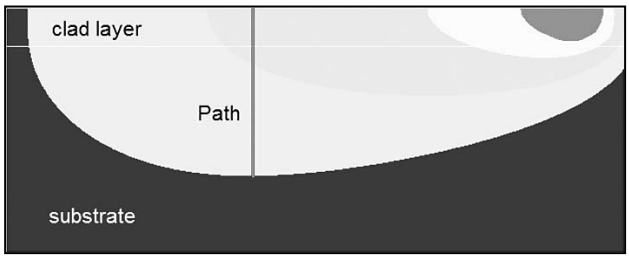

Fig. 13 Shape of HAZ on the substrate.

Based on the depth of HAZ values it can be concluded that with constant power if the speed is increased less will be the HAZ.

5.4 Effect of process parameters on temperature distribution

Fig. 15 shows the temperature distribution across the clad layer. Temperature distribution at the time of deposition forth clad layer is plotted across the clad layer number. Slower the speed more will be the heat developed across the layers and at higher speed it will be less. When cladding with speed of 400 mm/min maximum temperature is 2895°C at fourth clad layer and minimum temperature is 680°C at bottom of clad layer one. When cladding with speed of 750 mm/min maximum temperature is 1820°C at fourth clad layer and minimum temperature is 325°C at bottom of clad layer one. From the graph with speed of 400mm/min it is melting the preceding clad layer completely and with speed of 500mm/min producing the melting temperature (1260°C) till the middle of the preceding clad layer.

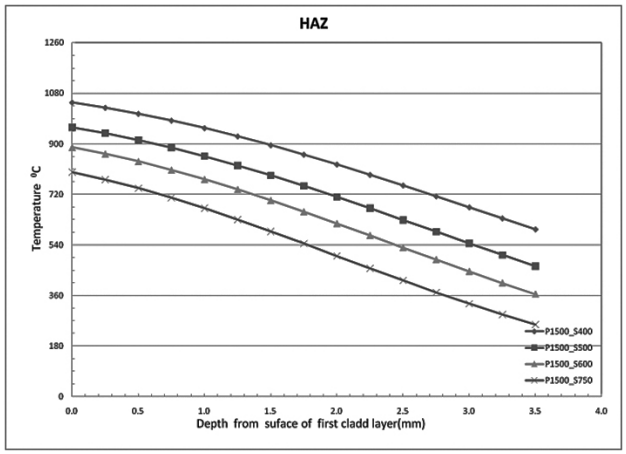

Fig. 14 Variation in depth of HAZ with different parameters.

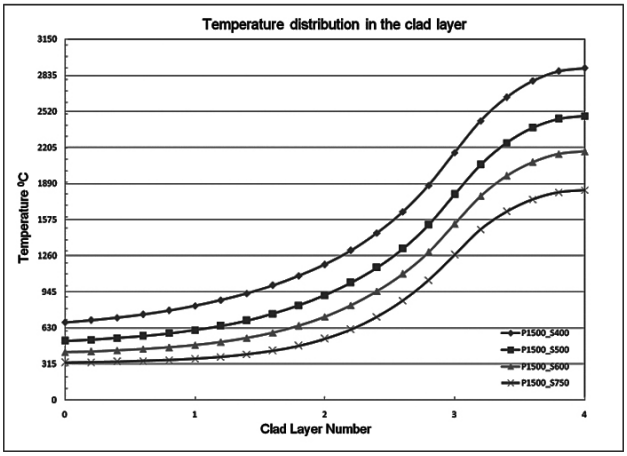

Fig. 15 Variation in Temperature with Layer number.

Table 4 Depth of heat affected zone for different parameters

Parameter	Depth of HAZ (mm)
P 1500 S 400	2.7
P 1500 S 500	1.95
P1500 S 600	1.35
P1500 S 750	Less than the depth of clad

5.5 Effect of process parameters on equivalent stress distribution across the clad

Based on the mechanical analysis it is observed that the value of equivalent stress across the clad layer is negligibly small. It varies from 21.9 to 45 MPa. This is due the geometry of the substrate. It will allow the deposited clad layer to expand or contract freely during the cooling time. So the internal stress generated during the cladding will be almost eliminated. So it can't be considered as criteria for optimization in this particular case. Again for the comparison of the different parameters these values were plotted across the depth of clad layer. Fig. 16 is showing distribution of stress for different parameters across the clad layer.

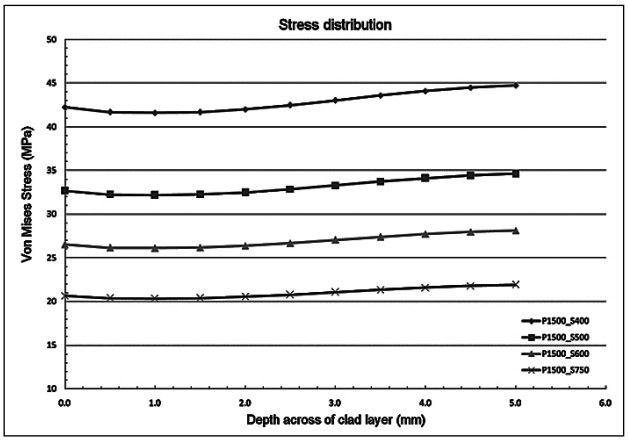

Fig. 16 Equvalent stress distribution for different parameters across the clad layer.

6. Experimental Verification of Simulated Results

The results of thermal cycles, dilution, HAZ, temperature across the clad layers and equivalent stress are compared and analyzed. The results are summarized in the table 5. Based on comparison it is clear that parameter with 1500W power and speeds of 500mm/min and 600mm/min giving satisfactory results in all the case. When the dilution value is considered, cladding with speed of 500mm/min giving more satisfactory result. So process parameter with speed 500mm/min and 1500W power is selected and initial run of cladding is performed.

The laser cladding was performed on nickel base alloy substrate material using 3kW CO_2 laser under argon atmosphere. The laser cladding was performed in the middle region of the substrate materials over a width of 2mm and length of 20mm as shown in Figure 17. The clad sample was cut and mounted for

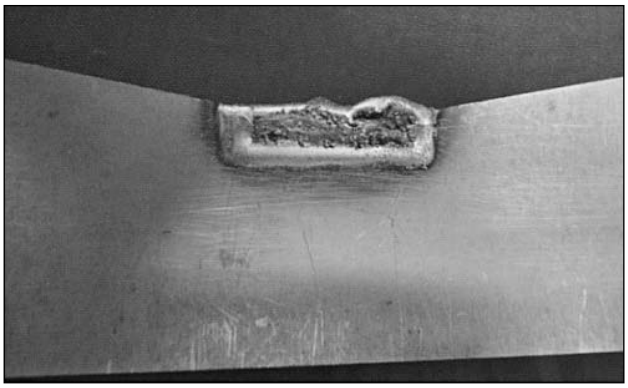

Fig. 17 Clad sample with power 1500W & speed 500mm/min

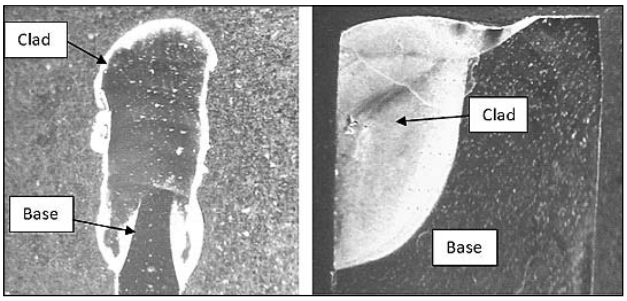

(a) (b)

Fig. 18 Macro images of clad sample at a) Cross section b) Surface region.

detailed examination. The images of laser clad cross sectional and surface region is shown in figure 18. This clearly shows that the clad specimen has not encountered with any defects like crack formation,

Table 5 Summary of Results Based on Primary Analysis

Process parameters	Melting of substrate	dilution %	Depth of HAZ	Temp. across clad layer(°C)	Equivalent Stress (MPa)
P1500 S400	more	37.5%	2.7	677-2898	41-45
P1500 S500	moderate	22.8%	1.95	515-2479	32.1-34.6
P1500 S600	moderate	9%	1.35	416-2170	26.1-28.1
P1500 S750	less	< 1%	-	326-1832	20.3-21.9

pore deposition or any more defects. It also shows that a fine metallurgical bonding is exists between substrate material and clad material.

7. Optimization of Parameters Based on Energy Density

From the initial analysis it is clear that parameter with 1500W power and speed of 500mm/min and 600mm/min giving satisfactory results and laser cladding is successfully performed with power 1500W and speed 500mm/min. So with the support of experimental and simulation results it can be confirmed that the energy density produced by these parameters can give a defect free clad. Based on this assumption energy density is calculated for these parameters based on the equation 7.1 and shown in table 6.

Energy density $E = \frac{4 \times p}{\pi d v}$ (9)

p = Laser Power (kW), d = Laser spot diameter in (cm), v = Processing speed (sec/cm).By keeping energy density in the range calculated above (11.5 – 9.5 kJ/cm2) five more new parameters are considered with different power and scanning speed (table 7). For checking the feasibility of the new parameters numerical simulation is carried out by repeating the same procedure.

Table 6 Energy density for initial parameters

Power (W)	Speed mm/min	Energy density (kJ/cm²)
1500	500	11.5
1500	600	9.5

Table 7 New parameters by keeping energy density from 10.3 to 11.1 kJ/cm²

Power (W)	Speed (mm/min)	Energy density (kJ/cm²)
1250	465	10.3
1500	545	10.5
1750	625	10.7
2000	700	10.9
2250	775	11.1

After simulation with second set of parameters dilution, HAZ and temperature distribution values are compared. The parameters with power 1750W speed 625mm/min, power 2000 speed 700mm/min and power 2250 speed 775mm/min showing a satisfactory result when dilution values are considered. HAZ will be minimum with less power and less processing speed and more when the power distribution and speed is high it is also noted that at higher power distribution and speed, the heating of substrate is less compared to low power and scanning speed. With a low scanning speed temperature will be getting enough time to conduct and penetrate to substrate. So comparing HAZ, both extreme cases can't be considered. Comparing heat developed across the layers Slower the speed more will be the heat developed across the layers and at higher speed it will be less.

The results dilution, HAZ and temperature across the clad layers are compared and analyzed. The results are summarized in the table 8. Based on above discussion and comparison it is clear that parameter with power 1750W and a speed of 625mm/min giving satisfactory results in all the case.

Table 8 summary of final results

Parameter	Dilution (%)	Depth of HAZ (mm)	Temperature Distribution across the layers (°C)
P 1250 S 465	12.29	1.500	470.1 – 2189.3
P 1500 S 545	15.97	1.750	465.0 – 2328.5
P 1750 S 625	18.03	1.825	461.1 – 2440.4
P 2000 S 700	20.63	1.900	461.6 – 2546.1
P 2250 S 775	22.48	1.925	462.2 – 2634.9

8. Conclusions

In this study a three dimensional (3D) finite element (FE) coupled thermo-mechanical model is used to simulate the laser cladding of Nickel super alloy powder on nickel super alloy substrate using 3D conical Gaussian heat source. Effect of laser beam power and scanning speed on dilution, HAZ, and residual stresses are analyzed and the process is optimized. The adaptability of FE model is verified experimentally and then it is investigated that for a fixed energy density. Based on the experimental and simulation results, the following conclusions are drawn:

i. Simulation with power 1500W and speeds of 500mm/min and 600mm/min giving satisfactory results when dilution, HAZ and temperature distribution across the clad layer and stress distribution of different parameters are compared.

ii. The clad layers are free to expand after the process due to the geometry of the specimen.

Stress generated is negligible based on simulation results. So the influence of stress distribution for optimization of parameters is neglected.

iii. Experimental validation of the simulation is done by cladding the specimen with power 1500W and speed 500mm/min. Good cladding is observed and it was free from defects.

iv. Energy density is calculated with the power 1500W, speeds 500mm/min and 600mm/min. It varies between 11.5 - 9.5kJ/cm2. Based on simulation and experimentation result, it is concluded that by keeping the energy density in this range, a defect free clad can be produced.

v. Five new parameters are introduced by keeping energy density within 11.5 - 9.5kJ/cm2. After simulating the five parameters and comparing the results, cladding with power 1750W and speed of 625mm/min could give good result.

References

1. William M Steen, "Laser Material Processing," Springer-Verlag London Limited, 1991.
2. G.Palumbo, S.Pinto and L.Tricarico, "Numerical finite element investigation on laser cladding treatment of ring geometries," Journal of Materials Processing Technology, vol. 155, pp. 1443–1450, 2004.
3. Y. Lei, R. Sun, Y. Tang and Wei Niu, "Numerical simulation of temperature distribution and TiC growth kinetics for highpower laser clad TiC/NiCrBSiC composite coatings," Optics & LaserTechnology, vol. 44, pp. 1141–1147, 2012.
4. G. Zhu, A. Zhang, D. Li, Y. Tang, Z. Tong and Q. Lu, "Numerical simulation of thermal behavior during laser direct metal deposition," Journal of Advanced Manufacturing Technology, vol. 55, pp. 55:945-954, 2011.
5. M. Hao and Y. Sun, "A FEM model for simulating temperature field in coaxial laser cladding of TI6AL4 V alloy using an inverse modeling approach," International Journal of Heat and Mass Transfer, vol. 64, pp. 352–360, 2013.
6. W.C. Tseng and J.N. Aoh, "Simulation study on laser cladding on preplaced powder layer with a tailored laser heat source," Optics & Laser Technology, vol. 48, pp. 141–152, 2013.
7. J.T. Hofmana, D.F.deLangec, B.Pathiraj and J. Meijer, "FEM modeling and experimental verification for dilution control in laser cladding," Journal of Materials Processing Technology, vol. 211, pp. 187–196, 2011.
8. Suárez, J.M.Amado, M.J.Tobar, A.Yáñez, E.Fraga and M.J. Peel, "Study of residual stresses generated inside laser cladded plates using FEM and diffraction of synchrotron radiation," Surface & Coatings Technology, vol. 204, pp. 1983–1988, 2010.
9. N.SivaShanmugam, G.Buvanashekaran and K. Sankaranarayanasamy, "Some studies on weld bead geometries for laser spot welding process using finite element analysis," Materials and Design, vol. 34, pp. 412–426, 2012.
10. G. Zhao, C. Cho and J. Kim, "Application of 3-D finite element method using Lagrangian formulation to dilution control in laser cladding process," International Journal of Mechanical Sciences, vol. 45, pp. 777 – 796, 2003.

Life Cycle Reliability and Safety Engineering
Vol.3 Issue 4 (2014) 24-47

Role of Environment in Corrosion Induced Degradation of Electronic Systems: A Review

V.K.Tapas, P.V.Varde
Bhabha Atomic Research Centre, Mumbai, India 400085.
vktapas@barc.gov.in

Abstract

More than 50% of electronic system failure is due to the environmental conditions such as humidity, ionic or organic contaminants, atmospheric corrodents, temperature, residuals; etc. which can accelerates an electrochemical reactions and causes corrosion of microelectronic components. Corrosive gases and water vapours from humid condition come into contact with the base metal results in buildup of various chemical reaction products. Ionic contamination responsible for electrochemical reaction, forms soluble complexes with metals, it can degrade the protective oxide film that forms on the positively biased metallization and/or lead to change in the local pH. Deterioration of metal components of electronic circuitry due to electrochemical migration and whisker growth need to be controlled in order to reduce the corrosion. With explosive increase in demand and miniturization in microelectronics resulted in smaller components, closer spacing and thinner metallic path, it is expected that the corrosion and deterioration of microelectronic systems may become cause of concern. This paper presents a comprehensive review and summerises the current understanding of chemistry behind possible causes of corrosion of electronic devices and its failure mechanism.

Keywords: - Electronic devices, Failure mechanism; Reliability; Whisker Growth; Electrochemical migrations.

1. Introduction:

Electronic industry has seen growing evolution at brisk pace for the past several decades from thick to thin films and to ever increasing miniaturization. Spectacular scientific and engineering advances in electronics has great influence in our life, from all forms of communication to extremely delicate and sophisticated medical applications to super computers for defence and space exploration. With the invention of transistor in 1948 and integrated circuit chips soon thereafter, development in transistor technology continue to follow an exponential progress represented by Moore`s law- doubling the number of devices per chip every 18 months phenomenal reduction in size and increased performance in electronics are result of continuous developments in electronic materials, processing technologies and unique integration scheme [1]. Miniaturization of circuitry, which leads to products that perform faster and better, has been chiefly responsible for this revolution. Shrinking the electronic devices has yielded lower cost, expanded performance, and higher reliability.

Development of a electronics systems begin with a demand from industry which allows far greater compatible device to be built into many more everyday items, such as: computers, from inexpensive personal computers through business computers to powerful supercomputers; communications systems, including switching stations and satellite communications; consumer products, such as electronic watches, video games, and pocket calculators; control systems for industrial applications, automobiles, and home appliances and military systems for national defence. Each type of device requires circuit design, component arrangement, preparation of a substrate, and the depositing of proper materials on the substrate [2, 3]. These devices are made from semiconductors like silicon and germanium. Several components are available in microelectronic scale such as transistors, capacitors, inductors, resistors, diodes, insulators and conductors. Microelectronics can be divided to its subfields which in turn are connected to other micro related fields. These subfields are micro electromechanical systems, nanoelectronics, optoelectronics and single electron devices [4]

While electronics community continues to invent new solutions around the world to keep Moore's law alive and even to go beyond Moore with disruptive technologies, there is ever-increasing awareness, R&D effort that are based upon or derived from silicon technologies. Along with the technology development, the business trends of microelectronics are represented by cost reduction, shorter-time-to-market and outsourcing. However, as the demand for increasingly effective electronic systems continues, improvements will continue to be made in state-of-the-art electronics to meet the demands. In Large-Scale Integration (LSI) and Very Large-Scale Integration (VLSI) a variety of circuits can be implanted on a wafer resulting reduction in size and weight of the device. LSI and VLSI are the results of improved microelectronic production technology. In Complementary metal oxide semiconductor (CMOS) transistor is the most common transistor used in the industry owing to its ease of integration and low static power dissipation. A smaller size of components being used to manufacture microelectronics typically is too small for humans to efficiently solder onto printed circuit boards. Thousands of components can be placed per hour utilizing a surface mount technology machines to place each component efficiently on the circuit board. These automation makes the entire manufacturing process more efficient which also reduces the overall cost [5, 6, 7].

Intel Corporation researchers have achieved a significant breakthrough by building the world's smallest and fastest CMOS transistor. This breakthrough will allow Intel to build microprocessors containing more than 400 million transistors, running at 10 gigahertz (10 billion cycles per second) and operating at less than one volt. Smaller transistors are faster, and fast transistors are the key building block for fast microprocessors, and several other smart devices. These new transistors, which act like switches controlling the flow of electrons inside a microchip, could complete 400 million calculations in microseconds [8]. Microfluidic chips a new generation device fitted on smart handheld gadgets is effective equipments can be used by doctors in their clinical laboratories [9].

Many large universities in the world conduct research in electronics to make the components smaller than the existing size of the components .Thus, even as existing capabilities are being improved; new areas of electronic use are being explored [10]. With the aggressive scaling of advanced integrated circuits (ICs) to deep submicron levels, the signal delay caused by interconnects became increasingly significant compared to the delay caused by the gate [11, 12,]. To suit the needs of those who use the products based on microelectronic devices, intensive research and several efforts have been carried out in microelectronics aimed at making circuits more reliable. The circuit should have a less power requirement and minimum heat is to be generated. These goals are prioritized in different ways depending on the end use. When selecting the most useful packaging technique, its environmental and electrical performance and the maintainability aspects are to be considered.

2. Microelectronics Reliability

Reliability of a system or component is defined as the ability to perform its required function under given conditions for a specified period of time [13]. The concerns for reliability of electronic components are driven by two major trends in the current electronics industry [14, 15, 16,]. The first trend is to accommodate a large number of circuits on a single chip. This involves the increase of packaging density of electronic circuits, the decrease of size and weight of associated elements and structures, and the increase of connection numbers in individual systems. The second trend is to implement lead-free soldering techniques in electronics industry, solder joints connect different electronic elements. Failure indicates the device non-operational due to damage caused by a failure mechanism, generally accelerated by external and/or internal stresses [17, 18,]. The microelectronic system components reliability is evaluated by a variety of established isothermal and thermal tests based on relevant standards [19, 20, 21,]. Design rules, operating voltage, and maximum switching speeds are selected to ensure functional operation over the intended lifetime of the product.

To determine the ultimate performance for a given set of design constraints, reliability must be modeled for its specific operating condition. Reliability modeling for the purpose of lifetime prediction is, therefore, the ultimate task of a failure evaluation. Over the last several decades, physical behavior of the critical failure mechanisms in electronic devices has grown significantly. Confidence in historical reliability models has led to more aggressive design rules that have been successfully applied to the latest Very Large Scale Integration technology. One result of improved reliability modeling has been accelerated performance; that is, performance beyond the expectation of Moore's

Law. A consequence of more aggressive design rules has been a reduction in the significance of a single failure mechanism. Hence, in modern devices, there is no single-failure mode that is more likely to occur than any other within a range of specified operating conditions. This is practically guaranteed by the integration of modern simulation tools in the design process. The consequence of more advanced reliability modeling tools is a new awareness that device failures result from a combination of several competing failure mechanisms.

The exponential, or constant failure rate (CFR), model [22] had been used in 1980`s for describing the useful life of electronic components. During the 1980s and early 1990s, with the introduction of integrated circuits (ICs), more and more evidence was gathered suggesting that the CFR model was no longer applicable. In the 1990s, attempts were focused on finding an electronic system reliability assessment methodology, including causes of failures, that could be used in the design and manufacturing of electronic systems. To cover the vast range of electronic devices, the concept called "similar-system" was introduced which refers to a system that uses similar technology and is built for similar application, or performs a similar function [23]. The next step was to find whether the "similar-system" was used for existing field data. The data from a predecessor system could be used to generate the prediction of a new "similar-system" to the extent that the new generation was evolutionary [24]. These reliability device simulators successfully model the most significant physical failure mechanisms in modern electronic devices, such as time-dependent dielectric breakdown, negative bias temperature instability, electromigration and hot carrier injection. These mechanisms are modeled throughout the circuit design process so that the system will operate for a minimum expected useful life [25, 26, 27, 28].

Accelerated life tests (ALTs) provide a consistent basis for the prediction of the probability of failure after the given time of service. This information can be extremely helpful in understanding the reliability of the product and its viable design. Therefore accelerated life tests, along with the (accelerated) product development/verification tests and qualification tests should play an important role in understanding and predicting the short- and long-term reliability of microelectronics equipment and devices. Generally for an accelerated test an Arrhenius model has been widely applied at high temperatures to evaluate the product reliability data in a reasonable amount of time. By exposing the devices to elevated temperatures, it is possible to reduce the time to failure of a component, thereby enabling data to be obtained in a shorter time. Such a technique is known as "accelerated testing'' and is widely used throughout the semiconductor industry. The rate at which many chemical processes take place is governed by the Arrhenius equation.

$$R = A\ exp\left(-\frac{E_a}{kT}\right) \quad (1)$$

Where,

R = Rate of the process, A= α proportional multiplier, E_α= Energy of activation,

k= Boltzmann's constant,

T = Absolute temperature in Kelvin.

While the Arrhenius model emphasizes the dependency of reactions on temperature, the Eyring model [29] is commonly used for demonstrating the dependency of reactions on stress factors other than temperature, such as mechanical stress, humidity or voltage.

$$t_f = AT^{\acute{\alpha}}\ exp\left\{\frac{\Delta H}{kT} + (B+\frac{C}{T})S_1\right\} \quad (2)$$

Where, *t_f is the life characteristic related to temperature and another stress. A, α, B and C are constants. T is absolute temperature. S_1 is a stress factor other than temperature.*

A set of parameters for failure mechanisms and major wearout were identified and the algorithms of extracting these parameters for a given technology were developed by accelerated tests on test structures. A circuit simulator, such as SPICE [30, 31], was employed to calculate the electrical parameters of fresh and degraded devices to predict their degradation or failure from these parameters. In the simulation, an Age parameter was calculated for each device with the following formula:

$$Age\ (\tau) = \int_{t=0}^{t=\tau}\left(\frac{I_{sub}}{I_{ds}}\right)^m \frac{I_{ds}}{WH}\,dt \quad (3)$$

Where,

W is a width of the transistor; m and H are technology dependent parameters determined from experiments; I_{sub} is the substrate current; I_{ds} is the drain current; s is the time for stress [32].

This reliability simulation method can help designers to understand the devices degradation within the circuits and make design compromise between performance and reliability in the product design stage.

3. Major Microelectronic Components

3.1 Interconnects

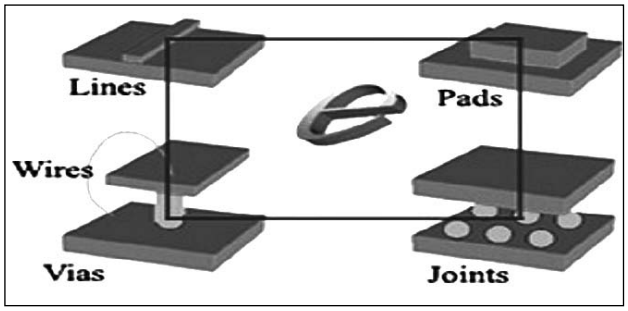

Fig.1: Interconnects
(Image courtesy: www.synl.ac.cn/org/mic/)

Interconnects may consist of conductive lines, pads, vias, wires and joints that form interconnected networks. Signal transmission along the interconnects has become increasingly important in limiting the speed, the size, the functionalities, and the reliability of modern microelectronic devices. In recent years, more integration and performance demands have required use of the alloys of copper, silver, tin, gold, zinc and nickel to form interconnects at various levels of the device [33, 34]. Current density in interconnects can reach values of 1-2x10^5A/cm^2 during device operation at 125^{0}C. Metal like copper offers low electric resistivity, high thermal and electric conductivity, easy fabricating and joining, and wide range of attainable mechanical properties have made copper as one of main materials in electronic packaging [34,35,36]. However copper corrosion can occur during the copper interconnect manufacturing processes due to its exposure to the chemical or ambient environment. In aqueous environments at ambient temperature, a thin layer of Cu_2O forms first on the copper surface by the oxidation and reduction reaction. The growth of the Cu_2O takes place on the top of surface through the mass transport of the Cu+ ions and electrons in a direction normal to the surface via vacancies [37, 38, 39].

The second stage of oxidation, the formation of the CuO from Cu_2O is usually a slower process. It is governed by the in-diffusion of oxygen into the oxide.

$$4Cu + 2H_2O \rightarrow 2Cu_2O + 4H^+ + 4e^- \quad (4)$$

$$O_2 + 2H_2O + 4e^- \rightarrow 4(OH)^- \quad (5)$$

$$2Cu_2O + O_2 \rightarrow 4CuO \quad (6)$$

$$4H^+ + 4(OH)^- \rightarrow 4H_2O \quad (7)$$

The primary effects of copper oxidation in copper interconnection wires and copper lead frames are,

1. Copper oxidation at the interface of Cu-Al bonding area causes the cracks, decreases the interfacial shear strength, and weakens the Cu-Al bonding [40].
2. Copper oxidation in the area of the copper lead frames die pad and molding compound causes the delamination of packages [41].
3. Copper oxidation induces poor adhesion in the area of copper lead frame and molding compound so that the moisture is able to penetrate through the crevices creating corrosion problem in packages [42].

To mitigate the corrosion of copper, corrosion inhibitor, such as Benzotriazole (BTA), can be prominantly used during manufacturing process of electronics. Corrosion of copper, particularly due to photovoltaic effect can be reduced using the dark environment during the manufacturing process. Forming a higher corrosion resistant layer or layers with a displacement plating process at the top surface of the copper interconnects can be helpful to reduce or eliminate the problem. For example, the metal used for the displacement plating layers may be Palladium, Platinum, Rhodium, Ruthenium, Gold, Silver, Lead, Nickel, Cadmium, Tin, or other noble metals and their alloys. The use of displacement plating to selectively coat copper interconnects with higher corrosion resistant metal or metal alloy layers during the manufacturing process of copper interconnects will minimize the occurrence of copper interconnect corrosion[43].

3.2 Connectors

Connector provides a separable connection between two elements of an electronic system without unacceptable signal distortion or power loss. Corrosion of connectors relates primarily to the contact interface and the contact finish. The contact interface consists of parallel resistances of metallic and film covered regions. Corrosion increases contact resistance by a series contribution due to films at the interface and a reduction in contact area due to penetration of corrosion products into the interface. In case of *Edge Connectors,* Contacts may be made solely of copper or gold-plated over a nickel-plated copper substrate, and are both susceptible to corrosion. A thin layer of gold plating is provided over the conducting surface of the PCB to ensure that the electrical contact between the board and the connector is maintained with the highest

integrity over a long period of time**.** Noble metal like gold, palladium and alloys of these metals and non noble metal primarily tin or tin/lead provide corrosion protection for the base metal. Noble finishes minimize film formation, while for tin finishes the surface oxides are easily disrupted [44].

Electroplated hard gold is most widely used as a contact finish for connectors. Commonly employed hard gold plating baths contain $KAu(CN)_2$ as the source of gold,a citrate buffer of pH 3.5 to 4.0 and a small amount of a Co or Ni salt as the hardening agent. Those baths abbrivated as CoHG and NiHG. Palladium and palladium alloys, especially Pd-Ni and Pd-Co, capped with a thin layer of hard gold are also employed as contact finishes [45, 46, 47, 48]. Compared with various properties of hard gold (NiHG), Pd-Ni and Pd-Co deposits, it was shown that both hardness and wear resistance increases in the order NiHG < Pd-Ni < Pd-Co, which clearly indicate the superiority of the palladium alloys compared to NiHG [48]. The small grain size of the hard gold is attributed to the inhibition of crystal growth caused by incorporated impurities or inclusion.

3.3 Solder

Soldering provides electrical, thermal and mechanical continuity in electronics assemblies, it is a well-known metallurgical joining method and material with a melting point below 425°C is used for solder joints [49]. It also serves as a path for dissipation of the heat generated by the semiconductors. Oxidation of solder alloys depending upon the environments in which solders are placed, the extent of oxidation can be controlled by restricting the oxygen content in the environment so that the oxidation can be kept to a minimum. It is essential to use H_2 as reducing gas to prevent further oxidation. Thermodynamic free energy ΔG^0 of oxide formation determines whether an oxide film will form spontaneously for a given set of environmental conditions [50, 51]. The solder is thus not only exposed to air, but also moisture and other corrosives such as chlorine and sulphur compounds. In addition, solder alloys are electrically connected with other metallic components in the electronic device, most notably the copper conductors. Therefore, there is also the potential for galvanically induced corrosion of the solder, which could aggravate any atmospheric corrosion that might be occurring.

Corrosion of solder alloys, in the presence of a suitable electrolyte can occur either due to the potential difference between the major phases in the alloy or galvanic coupling between one or more phases of the alloy and other parts of the devices. The corrosion behavior of 52In-48Sn soldered on Au substrate in the presence of 15-25 ppb Cl_2 at 85°C and 85% relative humidity was studied by Abtew [52] and the corrosion product was identified as $In(OH)_3$. Vincent and Richards [53] tested Bi, Zn, Ag, Cu, and Sb with Sn eutectic in an environment containing 200ppm NO_2, 100 ppb H_2S, 20 ppb Cl_2 at 30°C and 70% relative humidity. In case of Sn-9Zn precipitation of $ZnCl_2$ were observed. If Δemf between the phases present in the solder alloy is large, corrosion is likely to take place because the electrochemical coupling in the presence of moisture is high. Some metals such as Cu, Au, Ag, Ni, and Pd are frequently used in microelectronic with various compositions.

The most widely used Pb-Sn solder has the eutectic composition. In the electronics industry, the lead generated by the disposal of electronic assemblies is considered as hazardous to the environment because of lead's toxicity. In 1986, a review of the use of lead in electrical and electronic applications actually revealed a dramatic decrease. The use of lead for electronic soldering accounts for approximately 40-50% of the total for all soldering uses. It is expected that industries will be required to increase the extent of recycling of lead. But the use of recycled lead for electronics application displays higher ά-particle emission than virgin lead [54] .This can have detrimental effects on the performance of integrated circuits because ά-particle emission leads to the occurrence of soft errors. Therefore, developing viable alternative Lead-free solders for electronic assemblies is of paramount importance.

There are several Pb-free solders, such as Sn-Au, Sn-In, Sn-Ag, Sn-Bi, that have been in use in the electronics industry for special applications. A relatively large number of Pb-free solder alloys with their elemental compositions are summarized in the Table 1. Lead, Zinc, Copper, Antimony, Bismuth, Tin, Silver, Indium are also major elemental metals used in solders. The solder alloys listed below are binary, ternary and some are even quaternary alloys. It can be noticed that a very large number of these solder alloys are based on Sn being the primary or major constituent. The two other elements that are major constituents are in and Bi. Other alloying elements are Zn, Ag, Sb, and Cu.

Table 1: Pb free solder with their elemental compositions.

Alloys	Sn	In	Zn	Ag	Bi	Sb	Cu
2Sn-58Bi	42.0				58		
77.2Sn-20In-2.8Ag	77.2	20		2.8			
85Sn-10Bi-5-Zn	85		5		10		
91Sn-9Zn	91		9				
90Sn-7.5Bi-2-Ag-0.5Cu	90			2	7.5		0.5
96.3Sn-3.2Ag-0.5Cu	96.3			3.2			0.5
95Sn-3.5Ag-1.5In	95	1.5		3.5			
96.2Sn-2.5Ag-0.8Cu-0.5Sb	96.2			2.5		0.5	0.8
96.5Sn-3.5Ag	96.5			3.5			
98Sn-2Ag	98			2			
99.3Sn-0.7Cu	99.3						0.7
97Sn-2Cu-0.8Sb-0.1Ag	97			0.1		0.8	2
95Sn-5Sb	95					5	

4. Chemistry behind Corrosion

Corrosion is defined as the deterioration of a base metal resulting from a reaction with its environment. Corrosion essentially involves an electrochemical process and the basic requirements for electrochemical corrosion include electrically conductive anode, cathode, interconnecting electrolyte (humidity environment) and driving force. The driving force for electrochemical corrosion is the difference of electrochemical potentials between anode and cathode. The driving force can result from coupling of two dissimilar materials, on concentration gradient or externally applied electrical bias [55, 56]. Degradation process can occur rapidly or over many years depending on the particular concentration level and combination present at a site. As the chemical reaction continue, these corrosion product can form insulating layers on circuits which can lead to thermal failure or short circuits, pitting and metal loss can also occur. There are two aspects to analyse any type of corrosion reaction viz. thermodynamic feasibility and its kinetics. Driving force gives the thermodynamic feasibility and kinetics is determined by the variables of the system.

The electrochemical corrosion kinetics (rate) depends on various factors such as area ratio of anode to cathode, the polarization resistance of anode and cathode, conductivity of electrolyte solution, solution pH value, temperature, contamination, and driving force. Small anode and big cathode system corrodes much faster than big anode and small cathode. For instance, gold is deposited onto aluminum pad to prevent aluminum from corrosion. If defects of deposit gold layer exist and small area of fresh aluminum is exposed to the corrosive environment, aluminum gets corroded much faster because of small anode of exposed aluminum and big gold deposit layer around. The most common and important electrochemical reaction between the metal and its surrounding environment can be explained by the following reaction. Corrosion of metal occurs as a result of chemical reaction between the metal M and moisture. A simple anodic oxidation/reduction corrosion reaction takes place,

$M \rightarrow M^{n+} + ne$ *Oxidation* (8)

$2H_2O + 0_2 + 4e^- \rightarrow 4\ OH^-$ *Reduction* (9)

$M^{n+} + n\ (OH) \rightarrow M\ (OH)\ n$ *Corrosion Product* (10)

In general it has been obsreved that the corrosion of aluminium is the most common failure mechanism in microelectronic device. The electrolysis of water which produces hydroxyl and hydrogen ions is given by an anodic reaction specifying the oxidation of water.There are three general reactions [57] by which aluminum may react anodically in the presence of water.

Dissolution of metal takes place at Anode

(a) At low pH value,

$Al \rightarrow Al^{3+} + 3e^-$ (11)

$Al^{3+} + 3H_2O \rightarrow Al\ (OH)_3 + 3H^+$ (12)

(b) From weak acid to neutral pH range.

$2Al^{3+} + 3H_2O + 6e^- \rightarrow Al_2O_3 + 6H^+$ (13)

(c) At some high pH (high alkaline solution))

$Al + 2H_2O + 3e^- \rightarrow AlO_2^- + 4H^+$ (14)

Following reactions takes place at cathode:

(a) Evolution of hydrogen from solutions.

$3H^+ + 3e^- \rightarrow \frac{3}{2} H_2$ *(acid solution)* (15)

$2H_2O + 2e^- \rightarrow H_2\uparrow + 2\ OH^-$ *(neutral/alkaline)* (16)

Creation of H^+ ions leads to a more acidic (pH <7) environment near the anode, while the creation of OH^- leads to more basic environment (pH>7) near the cathode. The local pH strongly influences the corrosion behaviour of metals, preventing the charge transfer by minimizing current flow between the anode and cathode is therefore an important consideration in prevention of corrosion. The corrosion product of aluminum is usually believed to be Al $(OH)_3$ in the microelectronic packaging because the moisture environment is usually weak acid or neutral, but it actually depends on the pH value of electrolyte solution and activity of aluminum ions in the solution. It has been observed that the corrosion activity for Al is relatively low and is nearly independent of the applied voltage, the strong native oxide (Al_2O_3) on aluminium serves as a self-passivation layer.

In order for the corrosion to continue at a rapid rate, the ions must be able to diffuse rapidly to and from the regions of oxidation/reduction. However, for dry or ambient corrosion, the activation energy for diffusion is generally higher and the corrosion rate is very dependent on the percentage relative humidity (%RH).

5. Case Study

Example of Field failure:

In Light Water Cooling System of Power Reactors, a generation of liquid waste takes place due to the regeneration activities of various ion exchange columns. The liquid wastes are chemical in nature which consists of several corrosive products. Depending up on the quality of liquid waste, these effluents are sent in to respective annular sumps and treated with either acid or alkali before its final disposal into the Sea. Annular sumps are equipped with microprocessor level controllers for giving alarm when the sump is full. Regular inspections of these devices showed a severe corrosion on the surface of the circuit board. Failure of circuit system was found to be significantly higher due to frequent regeneration activities of ion exchange bed with Sulphuric acid. In this board metallurgy, the plating left significant amount of exposed copper which then react with sulphur compound causing bridges between the leads of components and system failures. The corrosion product is clearly composed of a copper and sulphur compound which is shown in figure 2.

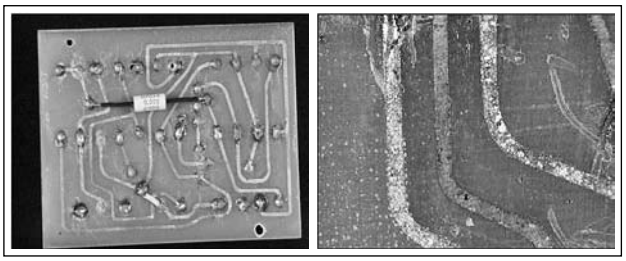

(a) (b)

Fig.2: *(a) Corrosion found on circuit board after exposure to high elemental sulphur environment.*
(b) Prominent deposition of green hydrated copper sulphate residues on circuit track.

Air oxidation of Cu form cuprite (Cu_2O) which gradually oxidise further to the black oxide (CuO) and black sulphide (CuS) products. The black layer of CuO and CuS slowly react with sulphur dioxide and carbon dioxide again in presence of moisture in the atmosphere to form green hydrated copper sulphate $Cu_4SO_4(OH)_6$. Reactions are as follows

$$2Cu + O_2 \rightarrow Cu_2O \quad \text{oxidation of Cu by } O_2 \qquad (17)$$

$$2Cu_2O + O_2 \rightarrow 4CuO \quad \text{oxidation to Cu (II) oxide} \qquad (18)$$

$$Cu + S \rightarrow CuS \quad \text{oxidation to Cu (II) sulphide} \qquad (19)$$

CuO and CuS slowly reacts with carbon dioxide (CO_2), sulphur trioxide (SO_3) and hydroxide ions (OH^-) in water from the air to eventually form $Cu_2CO_3(OH)_2$ and $Cu_4SO_4(OH)_6$.

$$2CuO + CO_2 + H_2O \rightarrow Cu_2CO_3(OH)_2 \qquad (20)$$

$$4CuO + SO_3 + 3H_2O \rightarrow Cu_4SO_4(OH)_6 \qquad (21)$$

The extent of humidity and sulphur related air pollution has significant impact to form green hydrated copper sulphate $Cu_4SO_4(OH)_6$.

6. Corrosion and Failure Mechanism

Corrosion of metal is a chemical reaction caused primarily by attack of gaseous contaminants and is accelerated by heat and moisture. Rapid shifts in either temperature or humidity cause small portions of circuits to fall below the dew point temperature, thereby facilitating condensation of contaminants. Relative humidity above 50% accelerates corrosion by forming conductive solutions on a small scale on electronic components. Microscopic pools of condensation then absorb contaminant gases to become electrolytes where crystal growth and electroplating occur. Above 80% RH, electronic corrosive damage will occur regardless of the levels of contamination.

Contribution of various acidic gases such as hydrogen sulphide, sulphur and nitrogen oxides,

chlorine and hydrogen fluoride, caustic gases such as ammonia and oxidising gases such as ozone can cause corrosion of electronic equipments, acidic gases are typically the most harmful, for instance it take only 10 parts per billion (ppb) of chlorine to inflict the same amount of damage as 25,000 ppb of ammonia. Various contaminants include fine and coarse particles of species such as chloride, sulphates, sodium, ammonium, potassium, magnesium and calcium. Presence of these ionic contaminants can accelerate de-lamination. Once the de-lamination occurs, moisture can absorb or condense on to the surface of the microelectronic device. The de-lamination creates surface leakage paths in an area of the device where two metal interconnection lines reside at two different potentials. The surface leakage current leads to metal oxidation at the anode in the form of M^+ ions and to reduction of water at the cathode in the form of hydroxyl ions $(OH)^-$ shown in fig 3. The metal ions can oxidise near anode and form a passive oxide film that protects the underlying metal from future corrosion.

However, if the pH is low or halide ionic contaminants are present then this passive oxide can break down, leading to further corrosion. If the oxidation of the metal ion formed at the anode does not occur then the metal ion can migrate towards the cathode and form a soluble salt.These contaminants can also form soluble complexes with metals resulting in dendrite formation and destroy the protective oxide film that forms on the positively biased metallization and/or lead to change in the local pH. Ionic contaminants commonly found on the die surface include chlorine from the encapsulants, phosphorus from the passivation, bromine and antimony trioxide

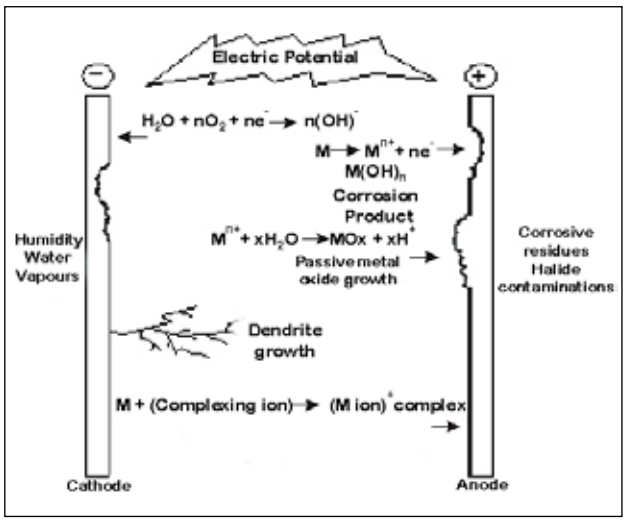

Fig.3: Schematic Diagram shows a variety of the most common Corrosion induced reaction that can lead to device failure.

from the flame retardants and sodium and potassium from semiconductor device processing. Therefore ionic contamination can have profound influence on the susceptibility of thin film metallization to corrosion [58, 59, 60, 61]. The presence of water and electrical bias is sufficient to initiate electrolytic corrosion.

Similar effects related to the formation of hydrolysed metal ions can also lead to device failure. The negatively biased interconnection line (i.e. the cathode) is also susceptible to corrosion. Failure occurs as a result of an open circuit. Alkaline contaminants lead to higher solution pH. They also tend to migrate to the cathode. Therefore they increase the susceptibility of the metal to cathodic corrosion induced failure [62, 63, 64]. It is necessary to minimise corrosive environment to eliminate the potential of destructive corrosion by metal migration. Destructive electrochemical migration occurs only under specific conditions. Growth of metal filament is initiated with the presence of an electrolytic solution dissolving metal ions in an electric field. Metal ions are electrodeposited along electrical leakage path forming a metal filament (dendrite) that may bridge the gap (short) between electrodes. The presence of the electrolytic solution across a potential at any environment results in as little as minor electrical leakage or as much as corrosive metal migration depending on the quantity of each of these factors. To understand the failure due to corrosion in polymer encapsulant with relative humidity and temperature, Time to failure t_f [65] is modeled as the sum of an induction time t_i and a time for the corrosion attack and failure t_c.

Therefore,

$$t_f = t_i + t_c: \tag{22}$$

The time required for a non-hermetic package to reach an external vapor pressure is

$$t_i = \frac{-4L^2}{\pi^2 D} ln\left(1 - \frac{P_{in}}{P_{out}}\right) \tag{23}$$

Where:

L is the length from edge of the chip to the outside of the package, D is the permeation constant, P_{in} is the inside partial pressure and P_{out} is the outside partial pressure.

The corrosion time is given by

$$t_c = \left(\frac{K_1 K_2 K_3}{K_4}\right)\left(\frac{w^2 hndF\rho}{4MVz}\right) \tag{24}$$

Where,

M is the atomic weight of a metal conductor,

d its density, n the chemical valence, V the voltage applied and ρ/z the sheet resistance of the electrolyte. K_1 is a measure of the resistivity to corrosion normalized to that of gold. K_2 is the coating integrity index and accounts for the existence and integrity of the passivation layer covering the diemetallization. K_3 is the duty cycle correction factor related to power cycling.

Thus the corrosion rate is decreased when the die temperature is increased by power dissipation. From above equation (eq.24) the environmental correction factor K_4, can be used to determine the time to failure for various temperature and humidity conditions. The K_4 term is modeled as

$$K_4 = \frac{(RH_R)^n}{(RH)^n} \frac{exp(E_a/K_{T_R})}{exp(E_a/K_T)} \quad (25)$$

Where:

RH_R and T_R are reference relative humidity (%) and reference temperature (K), respectively and n is a constant.

It has been observed among the environmental issues, a significant problem is the residue as well as the dust particles found on the circuit board. Residues are the contamination on the surface due to the remains of the chemicals used for manufacturing process, a small fractions of these chemicals are enough to accelerate the corrosion process. And the dust particles is another issue, which can acts as a moisture trapping agent, it may cause malfunctions by interrupting electrical contact between mating pairs of contact on connector or relays at relatively low humidity such as 50-70 % [66].

Whisker growth is an another phenomenon in electronics degradation, it is a filamentary growth reported to be a form of induced recrystallization related to metallurgical imperfections and occur under the influence of stress. Another type of failure involves the formation of metal bridges between two metal lines at different potentials which is associated with noble metals, such as silver and gold. In the presence of complexing contaminant, such as chloride residues from the package encapsulation polymer, soluble gold complexes form at the anode. These complexes diffuse from the anode to the cathode. At the cathode, gold complex is reduced to the metallic state and precipitate out of solution liberating the complexing ion. The ion will then under the influence of electric field, migrate towards anode. When it reaches anode it can participate once again in complex formation. When gold ion precipitates out at the cathode, there is small but real decrease in line to line spacing and therefore the local electric field which drives the process increases there. Thus the next gold complex that forms will be more likely to migrate to this location along the cathode. As this process continue, a dendrite forms. When the dendrite bridges the gap between the two metal lines, a short circuit is formed leading to a permanent failure or temporary device malfunction [67].

It is also possible for moisture-induced electrochemical degradation of the dielectric to occur if the current flowing through the dielectric is large enough, then the dielectric can corrode, changing its physical size and properties. This could lead to device failure. Silicon-based dielectrics, such as silicon nitride, silicon dioxide and alloys of two, are hydrolysed when exposed to moisture. These hydrolysed reaction products dissolved slowly in condensed water. Thus, if the solubility limit of dissolved silicon based reaction product is not reached before the dielectric is breached, then water can come in contact with the metallization and /or any underlying dielectric thin films such as phosphorus-doped silica. In such a way the susceptibility of the device to corrosion induced failure is increased.

Another possible corrosion induced metal loss is related to decrease in line width. The loss of interconnection cross-sectional area leads to an increased local current density. Since the electromigration resistance (i.e.current induced diffusion) decreases as the current density squared, it is possible that partial corrosion of a metal line will eventually lead to electromigration –induced device failure. The increase leakage could cause the device to fail. Finally local corrosion of small sections of the metallization can initiate arcing that leads to device failure [68, 69, 70, 71]. The damage to the microelectronic components resulting from corrosion attack is irreparable and compromising to the reliability of microelectronic devices.

7. Electrochemical Migration

Electrochemical migration (EMC) is a typical form of corrosion occurs due to the presence of a potential gradient between two susceptible conductors (Cu, Ag, Sn, Pb, etc.) connected by a thin layer of solution under ambient temperatures (<100°C) at low current densities (<1mA/cm^2). ECM involves the dissolution of a metal at the anode (oxidation reaction) and the transportation of the metal ions or conductive metal complexes formed along the moisture path to the

cathode (reduction reaction). At the cathode, these metal ions are reduced and deposited as pure metal, which then grows back toward the anode in the form of dendrites [72]. Metal compounds with low solubility product give fewer ions for migration, while those with high hydrogen overvoltage will not deposit.

The signature metallic dendrites, conductive anodic filament (CAF), and colloidal staining are all manifestations of electrochemical migration have been observed in microelectronic device. Growth of dendrites shown in Fig.4 finally leads to electric short between two points, which cause component failure or malfunction. An electrical failure in the device occurs as a result of either an open circuit due to the dissolution of the metal anode or a short circuit arising from the cathode-to-anode bridging of metallic dendrites [73].

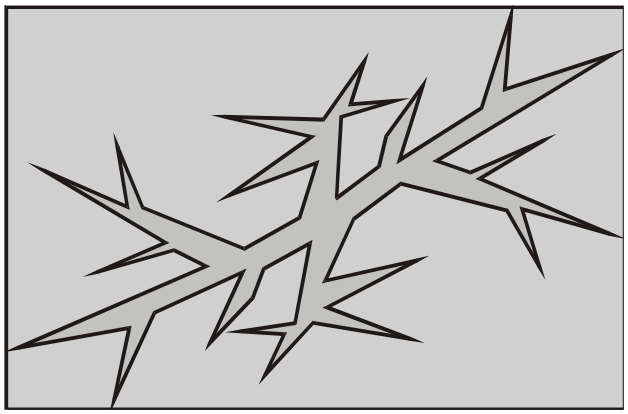

***Fig4**: Dendrite Growth: As the crystal grows, it tends to develop spikes and its shape changes into a tree like form.*

Thus transport of metal ions under the influence of an applied electric field primarily manifested as bridging metallic dendrites those results in electrical failures of microelectronic devices. Chazalviel introduced a 1D numerical model for ion transport in electrochemical deposition with only diffusion and migration as the transport modes. The model predicted the existence and behavior of a depletion layer next to the cathode [74].

Following this Fluery et al. described a model for electrochemical deposition (ECD) and ionic motion in which the growth speed of the metallic deposit equals the speed of anions withdrawing from the zone invaded by the metallic filaments. At every moment during growth, both cations and anions drift in the electric field in opposite directions; the cations meet the growing front and add on to it, while the anions pile up near the anode [75] as shown in fig 5.

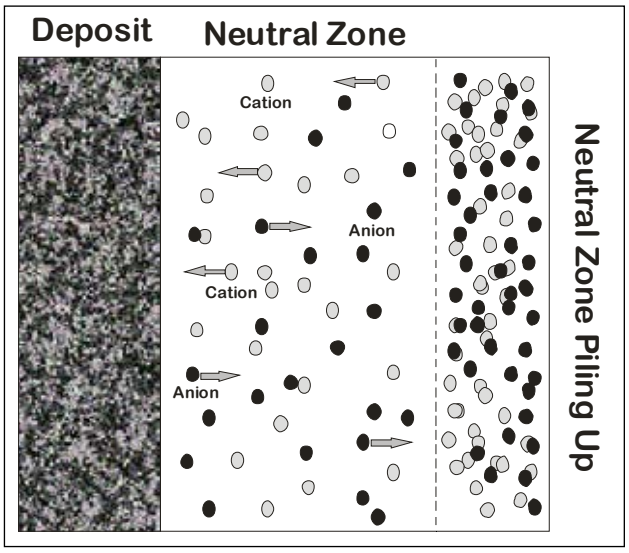

***Fig.5**: Schematic view of cation and anion concentration evolution during growth*

The front of the metallic dendrites is always rushing and remaining just behind the withdrawing anions. The zone enclosed between the filaments is completely depleted of ions of any kind. Fluery et al. also proposed that the Hecker effect, during the growth of the metallic deposits, is produced by changes in the solution due to positively charged impurities from the anode or encounters with zones of different pH. Initially, the impurities are on the edge of the anode but as the deposit grows, the impurities leave the anode, drifts in the bulk, and move toward the deposit. Initially impurities that reach and hit the growing dendritic front will induce a change in the morphology of the growing filaments. These are H^+ and OH^- ions impurities, in the context of H_2O molecules thereby providing a protonic drift; other impurities may also exists. Thus, maintaining the proper pH and controlling the impurities would enable to manage the dendritic morphology [75] and, consequently, mitigate the threat from ECM as filamentary-type dendrites are more dangerous than dense, compact dendrites. It has been observed that percolative moisture path, supply of migrating ions, and a bias voltage are the basic ingredients responsible for electrochemical migration to occur and device failures.

Contributing factors for dendrite growths:

i) Humidity

The duration of a percolative moisture path is a key factor in determining the mean time to failure (MTTF) of microelectronic devices. This moisture path can be broken (dried up), regenerated, or reformed as a different path, depending on the

ambient conditions. With relative humidity (RH) and temperature (T) under the same conditions, the MTTF remains somewhat similar and is independent of the onset of the bias voltage [76].

ii) Effect of Voltage

Since the minimum voltage required for water hydrolysis is 1.2 V, it is conceivable that below 1.2 V, little or no ECM activity may be expected. At higher voltage, however, more ions are made available as the pH drop due to water hydrolysis becomes conducive for metal dissolution [77]. When differently spaced conductor lines are biased together, there is a preferential propensity for dendrite/filament growth in regions of the narrowest spacings. This indicates that the critical electrical variable may be the voltage gradient (electric field) across the spacing. However, quantifying the electric field acting on the migrating ion is non-trivial due, in part, to the time dependency of the variables involved in the equation, i.e., branching and tortuosity of the electrolytic paths in the insulator and a constantly changing path length, ionic concentration, and conductivity [78].

iii) Temperature

The main effect of temperature is to increase conductivity, probably due to an increase in ion mobility with temperature and/or a decrease in the viscosity of surface solution. Higher temperature increases the susceptibility to ECM, especially when coupled with high relative humidity. Thus, an Arrhenius relationship is commonly used to model the temperature dependency of this failure mechanism.

$$MTTF_{ECM} \propto \exp\left(-\frac{E_a}{kT}\right) \quad (26)$$

iv) Effect of Ionic Contaminants

The ECM activity is directly proportional to the concentration of the ion impurities. The higher the ionic impurities, the more the metal-ion complexes formed and the faster these metals succumb to dendritic growth and short circuit. In certain corrosion-resistant metals (e.g., Au, Pd, and Pt), the presence of ionic impurities, especially chlorides (Cl^-), allows a series of complexation reactions to happen that will liberate the metal or metal–complex cations. Corrosion-resistant metal like gold can also be rendered susceptible to, an impurity-induced, electrochemical migration process. The discovery of gold dendrites inside ceramic packages leads to simulation experiments to induce their growth, it was found that the gold dendrites would grow only in the presence of all three factors, namely (i) bias voltage, (ii) hygroscopic nonylphenol (as the moisture trap or vehicle), and (iii) $Au(CN)_2$ (the complexation agent in the gold plating bath) [77,79,80]. The influence of ionic impurity is rather complex and involves various counteracting effects that change depending on the nature of the conductor and the concentration of the impurity ions.

v) Material and flux residue

Polymeric insulator materials (epoxies, phenolics, or silicones) used to protect microelectronic devices are non-hermetic and highly susceptible to moisture penetration. At any RH, the moisture absorption tendency of the microelectronics package is dependent on the surface condition of the insulator material [81, 82]. The main effects of absorbed moisture are moisture-induced plasticization and/or micromechanical degradation. The mechanical and chemical integrity of the epoxy is altered and deteriorates as a result of (i) microcrack formation from hygromechanical stresses, (ii) polymeric bond degradation due to chain scission, (iii) reduction of the glass transition temperature (Tg) due to plasticization, and (iv) degradation of polymer interfaces resulting in de-adhesion (delamination). As interfacial voids or delaminations are potential nucleation sites for capillary condensation, these can then provide an easy path for moisture ingression, i.e., a path of least resistance, to any available ambient moisture.

The nature of metal conductor surface also plays a role in determining the device susceptibility to ECM failure. Rough surfaces possess high-energy points that are ready targets for the migrating metal cations. In addition, metals that form tenacious metal oxides (e.g., Al_2O_3 and CuO) are certainly more protected against ECM than those having more soluble metal oxides (e.g., AgO). The flux residue is also one of the most deleterious process contaminants from the various assembly processes. Certain flux constituents, like the strongly hygroscopic polyglycols, greatly enhance the hydrophilicity of the epoxy. Polyglycol rapidly diffuses into the epoxy polymeric network at the assembly temperatures used and is retained within after the cleaning step. These become sites

for water condensation and a significant amount of moisture absorption can result if the critical humidity level is exceeded. These flux residues act either by modifying the epoxy surface and altering their moisture absorption propensity or, through a degradation process, becoming the source of moisture itself [78].

8. Whisker Growth

Whisker growth is believed to proceed either via a dislocation mechanism or through a grain growth /recystallization mechanism. Various factors such as crystalline structure, plating thickness, electroplating current density, substrate, temperature, humidity etc are responsible for whisker growth. Whisker growth as shown in Fig.6 can takes place in various types of metal surfaces, such as tin, zinc, cadmium, and antimony. Whiskers can be straight, kinked, hooked or forked and lumpy. Harsh environments may aggravate the problem by causing thermal and/or mechanical stresses in metal coated surfaces, leading to the growth of whiskers and its induced failures.

Fig 6: *A needle-like tin whisker.*

A common failure mode for whisker- prone electronic systems is whisker bridging, which causes electrical shorts. Whiskers often display a long (months and years) and unpredictable incubation period before significant growth occurs. High aspect ratio Sn whiskers are typically 1-5 μm in diameter and between 1-500 μm in length. The current worldwide initiative to reduce the use of lead (Pb) is driving the electronics industry to consider high tin alternatives to the widely used Sn-37Pb alloys used for plating and solder [83,84,85].

The spontaneous formation of tin whiskers suggests a decreased Gibbs free energy from the state of pure tin electroplate to the state of tin whiskers. This negative change of Gibbs free energy is the driving force of formation of tin whiskers. At the same time, Kinetic studies can provide the means to slow down the growth of tin whiskers, which are also helpful in dealing whiskers. Fig. 7 shows the relatiop between kinetics and thermodynamics.

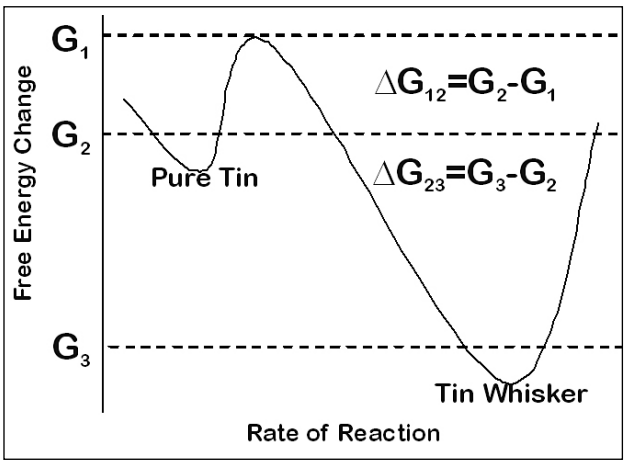

Fig 7*: Relationship of Kinetics and Thermodynamics [86].*

Here, ΔG_{12} is activation energy, which is the Kinetic reason and determines the growth rate of tin whiskers; the growth rate can be expressed as

$$\text{Growth Rate} = N \ln \left(\frac{\Delta G_{12}}{RT}\right) \quad (27)$$

Growth is highly variable and is likely to be determined by a complex relationship of factors including plating chemistry, plating thickness, substrate materials, grain structure, temperature, defects, diffusing coefficient, and environmental storage conditions. Growth rates from 0.03 to 9 mm/ yr have been observed in an integrated circuitary. ΔG_{23} is the change of Gibbs free energy; the spontaneous nature implies that the formation of tin whisker on pure tin plate is thermodynamically favorable.

Tin whiskers growth is generally believed to occur in order to relieve compressive stresses that exist within the pure tin plating. In general, growth is most likely induced by stresses such as those resulting from: residual stress within the tin plating, intermetallic compound formation, external stress, co-efficient of thermal expansion mismatches, surface and particle irradiation. Residual stresses are directly related to electroplating process and the materials properties that inherent from other pre-treatment, hence, the various factors that may increase stresses within tin plating are electroplating current density, grain size and shape, interfacial stress level, substrate stress levels, co-deposited carbon or hydrogen.

It was also noticed that the spontaneous development of compressive stress was responsible for diffusion of copper atoms from the substrate into the tin film and the formation of the intermetallic compound Cu_6Sn_5. Tin films with small grain size have more grain boundaries and provide diffusing species with more diffusion pathways. The amount of copper atoms diffused into tin grain boundaries per given time will increase with decreasing grain size, if given everything else same, compressive stress will build up more quickly in tin film with smaller grain and higher density of tin whiskers are expected (Figure.8). Moreover, the continuous growth of Sn whiskers must rely on grain boundary diffusion for mass supply [86]. Large number of grain boundaries is favorable also for this long-range diffusion of Sn atoms. Regarding to the shape of grains tin whiskers grow from the grains having different orientation from the major orientation of the tin film.

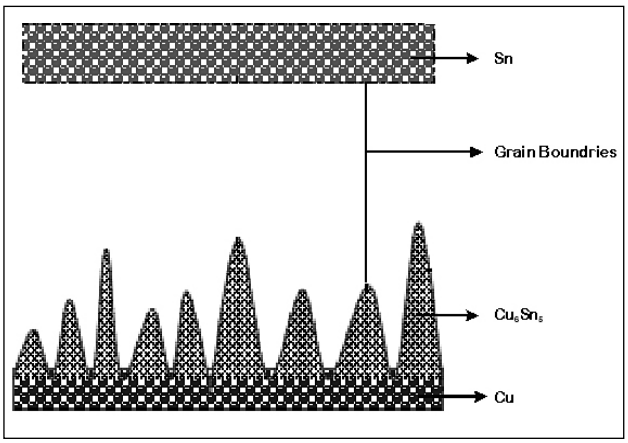

Fig 8: Cu_6Sn_5 Formed in Grain Boundaries within Tin. [86]

In this situation, the tin surface oxide film can be sheared along the boundaries of the grains. To release the compressive stress in the tin film, tin whiskers grow from the grain whose surface oxide is sheared [87]. It was inferred that with loosely packed grain boundaries, high angle have more dislocations to serve as diffusion paths, therefore, more prone to grow tin whiskers [88]. While other concluded low angle grain boundaries are more prone to whisker growth than high angle boundaries [89]. Due to the formation of intermetallic compound of Cu_6Sn_5 increases the specific volume and induces compressive stress within tin film. These intermetallic compound are considered as a flat layer formed between copper and tin, hence, it only give rise to compressive stress at the region near the interfaces. There are several analyses that are summarized as follows.

a) Diffusion via Grain Boundaries

If the intermetallic compound forms flatly in the interface between copper and tin, no stress will develop in the tin layer, regardless of the diffusion coefficients of species concerned. However, if the intermetallic compound layer forms in the tin grain boundaries, it will give rise to the compressive stress in the tin layer, because copper atoms are the dominant diffusing species. *B. Z. Lee* believes that the Cu_6Sn_5 layer is not flat and it penetrates into grain boundaries of tin film. This hypothesis is in agreement with the observation of tin whiskers only grow within tin film other than any interfaces [90].

b) Interstitial diffusion

Interstitial diffusion of copper atoms and the formation of intermetallic compound (Cu_6Sn_5) may alter the lattice spacing in the tin plating and generate compressive strain within tin lattice. *M.Endo* studied tin whiskers originated on a brass substrate where two diffusion species were found, zinc and copper. He believes that interstitial diffusion of copper into tin forms intermetallic compound and cause stress, while zinc atoms diffused toward the tin film surface and form oxide. This zinc oxide provides whiskers with sites to grow out of tin surface [91].

c) *Diffusion and surface oxidation*

When tin is deposited on a brass substrate, copper and zinc atoms from this substrate can both diffuse into tin film and forms Cu_6Sn_5 and zinc oxide as an intermetallic compounds [69]. Copper is more prone to stay within tin film and form intermetallic compound, while zinc atoms diffuse toward the tin film surface and bind there with oxygen to form oxide. More zinc atoms on the surface were found than that inside the tin film. *M. Endo* proposed that the formation of copper intermetallic compound may prevent further diffusion of zinc atoms from the brass substrate. Another study shows that zinc atoms have higher mobility than copper and could be more easily diffuse from brass substrate to tin surface than copper. The relatively solubility of zinc in tin implies that zinc atoms are the dominant and faster diffusing spices compared to tin [92].

d) Temperature

As the temperature rise the diffusion rate of copper into tin film can also increase which shows the quick build up of compressive stresses into

the substrate material, and accelerates the tin whiskers growth. However, high temperature also helps relief internal stress within tin film and consequently oppresses the formation of tin whiskers. Based on literature research, the optimum temperature for whisker to form is around 50 C°, and most of researches were conduct at this temperature. It was recommanded to use conformal coating or encapsulation that can protect electronic circuit. Contradictorily, in a conformal coating study, higher density of tin whiskers were observed on the samples stored under room temperature ambient conditions (25 C°) than that on samples stored at 50 C° [93]. Alloying as little as 0.9% lead with the tin dramatically reduces the density and growth rate of tin whiskers, but both nodular and filament whisker were observed at the compressively stressed area even for a 10% lead-tin finish in Cunningham`s experiments [94].

It was necessary to use Ni barrier effectively to reduce whisker growth, if the diffusion of copper species into tin films builds up internal stress eventually results in whisker growth, nickel barrier a barrierlayer may be an effective method to block the diffusion pathway and prevent whiskers. The nickel depositlower the initial stress between the interfaces and also act as an excellent barrier to copper diffusion, which hinders the formation of intermetallic compound [95]. Reflow is another effective process to minimise tin whisker, reflowing tin film with large grain size is less prone to grow whiskers, there is no compressive stress built up again in Sn film even after a long period of aging, e.g. 18 months, hence, no whisker growth observed [88].

9. Environmental effects on Corrosion

Environmentally humid condition results an accumulation of water and impurities on metal surfaces whereas heat and sunlight also decay the products and accelerate the process of corrosion and other harmful effects. Air velocity, temperature also has an effect on the rate of corrosion reaction and contamination of the surfaces. The weather averages of temperates and relative humidity during various seasons in Mumbai, India during the calendar year-2013 is shown in figure.9. The extremely significant factor to the corrosion risk is the relative humidity of the air exceeds 60% at all times. Corrosion and climatic effects increase the contact resistances of the joints, leakage currents between connectors and interconnects, increase in electromagnetic disturbances which can cause various operational faults of the circuit devices. At high temperature > 55°C, corrosion reactions accelerate even in dry conditions of use causing the decay of materials. Water, dust, gases and organic compounds cause leakage currents, short-circuits and mechanical changes. If the immediate environment of the device is relatively dust free and dry, relative humidity of the air is less than 40% then corrosion becomes so slow that it will not have much effect on the device.

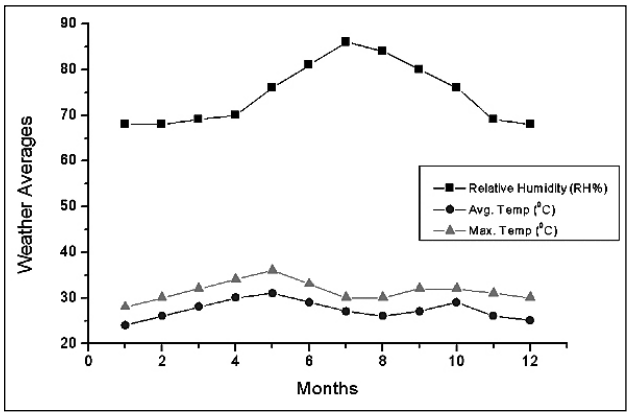

Fig 9: Weather averages of temperates during various seasons (Climate graph 2013 Mumbai, India)

The most common corrosion risk factor from environment is probably due to the soluble & insoluble salts from the sea water (chlorides) which can spread in the air as far as 50 km from the coasts. Considerable temperature variations can cause risk of water condensation on the surfaces whereby gases in the air and other impurities together with water form corrosive compounds, such as sulphuric, nitrogen and hydrochloric acids. These acidic substances on the surfaces of the components enhance corrosion reactions. Gaseous and ionic substances in the air and dust have basically spread evenly and everywhere in urban conditions. Concentrations exceeding the average considerably are only met in the vicinity of heavy traffic flows, industrial plants and power plants, which increase the risk for corrosion, form the usual. Electrical stress also speeds up corrosion, strong current can heat the solder joint and gradually weaken it. In dense wiring patterns the high field intensity between the wires increases leakage currents and accelerates corrosion on contaminated surfaces [96]. In microcircuits where the wire widths are in micrometres, metallic migration may occur (wire breakage) due to high density of the current and causes short malfunctions of the devices.

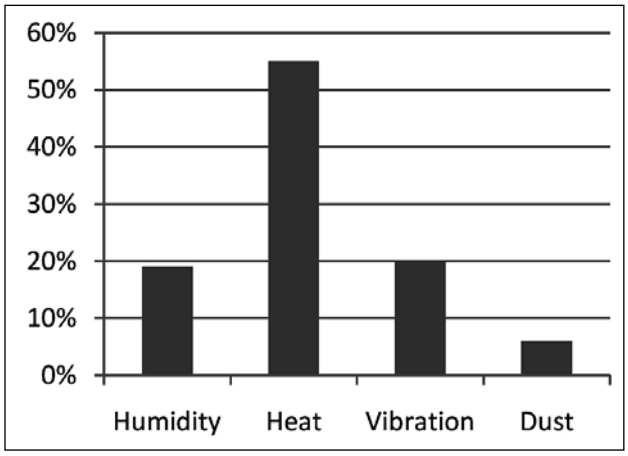

***Fig 10**: Reasons for failure of electronic devices (Courtesy: Flomerics, US Air Avionics Integrity Program, Journal of the IEST)*

The graph statistic (Fig.10) shows that majority of faults in electronics are related to heat, humidity and vibration. When conditions change, the faults may also disappear. The temperature readings cold/ hot, their fluctuation and humidity always affect the physical and chemical properties of materials and components. The material used in electronic devices is not completely inert (chemically passive) but the components, component boards and metal parts and plastic structures can be made relatively inert to the corrosive effects with reasonable work.

In most electronics, high temperature of use naturally dries the inside of the device, but accelerates oxygnation and decay of material which results in corrosion surfacing in another form, such as decay of the solder connections or embrittlement of insulators. On the other hand, effective cooling with rough or humid outside air increases the gas contacts and relative humidity of the air inside, which results in more corrosion and contamination in the contacts in the component leads. The electrochemical cell created on the surface of a metal always has a voltage difference between the anode (the corrosion area) and the cathode. If the voltage difference is less than 0.3 V then the rate of corrosion is slow. The failure mechanisms have different effect on different materials, the most common failure of the components can be observed with, connectors, interconnects, and a gradual decay of solder connections especially in hot spot. New devices also noticed thermal fluctuation and mechanical vibration in their frame structure causing breaks in wire connections and connectors.

There are various causes for occasional unidentified faults such as -reversible changing of component parameters due to change in the temperature, corrosion in the connections,leakage currents of surface of the component board in humid weather, leakage currents of soiled surfaces, breaks in connectors or wires due to thermal expansion, breaks due to vibration, contact faults caused by inferior contact spring material or design, stickiness of the keyboard due to chemicals of human origin, problems of the mechanical structure, software disturbance, disturbance in data transmission or power supply etc. These occasional faults are mentionaed below in Table No.2.

Table 2: Occasional failure of devices [125]

Classification of corrosion effects	
Electrical functionality	Change of series resistance in contacts, Breaks of conductors, Change of insulation resistance,Leakage currents, soiled surfaces Change of dielectric constant of materials,Faults of component packages,Faults of component leads Short-circuits, Breaks of cable
Mechanical Functionality	Increase of friction, Hindering of movement,Weakening of spring,Fault of contact mechanism,Fault of switch mechanism, Sudden breaks during heat and Mechanical Stresses
Mechanical strength	Break of mechanical actuator,Break of supporting structure,Break of solder joint
Appearance	Dusty appearance, Faults in outer surface, Color changes of platings, Soiled surfaces. Disappearance of markings
Malfunction	Intermittent failure, Groundless change of new component Rejection of nearly intact device, Failure of oftware, Fault in electric supply

It was noticed that the operation of electronic components get affected even before the corrosion products are produced. In dry and dusty conditions the air going inside the product contains a major concentration of oxygen and nitrogen whereas carbon dioxide, various nitrogen oxides, sulphuric compounds, sand dust, soot etc are also found in the low concentration. Such gases accumulate (adsorb) on the surfaces of the devices and also desorb (leave the surface) when the surrounding air flows across the surface and makes the surfaces conductive, which increases leakage currents and causes electric breakdown. Air pollutants such as sulphur dioxide,

hydrogen sulphide, oxides of nitrogen, chlorides have also been found to contribute to atmospheric corrosion [97]. Acidic gases, such as hydrogen sulphide, sulphur oxides, chlorine, hydrogen fluoride (HF) and nitrogen oxides are the most harmful gases that can pose problems to sensitive electronic equipments. These corrosive gases are generated primarily from auto emissions, heavy industrial production and heat and power generation. Weather conditions play a major role in concentrating or dispersing external gaseous contaminants. Industrial smoke contains both particulate and gaseous contaminants are a source of nitrogen oxide. Microfiche systems are heavy producers of ammonia, while printers can discharge sulphur compounds and chlorides. Gases often present at such low levels, are in sufficient amount to damage the microelectronic devices, hence most of the odor threshold levels are maintained much higher than the levels needed to cause corrosive damage [98,99,100].

The complexity and diverse nature of the atmospheric pollutants make the prediction of the atmospheric corrosion difficult. Inorder to derive corrosion, a direct approach to the problem is to measure the observed corrosion rates and the participating atmospheric parameters and correlate them. Rural environments generally are not aggressive towards metals. Urban atmosphere comprise of little industrial activity, characterized by pollution composed from motor vehicles and domestic fuel emissions which, with the addition of dew or fog, generate a highly corrosive wet acid film on exposed surfaces. Whereas industrial environment that spread sulphur oxides and nitrogen oxides produced by the burning of automotive fuels and fossil fuels in power stations are the major sources of corrosion. This contamination induces severe corrosion at relative humidities exceeding about 55%. This environment is characterized by proximity to the ocean and salt loded air that can produce severe corrosion damage of the metal alloys and accelerate deterioration of protective coating systems. Marine atmospheres are usually highly corrosive. The principal culprit in marine atmospheres is the chloride (Cl^-) ion derived from sodium chloride [101,102,103]. Pollutants which are commonly present in an atmosphere and its influence on metallic devices are given in table 3.

9.1 Active suphur compounds (H S)

Hydrogen sulphide (H_2S), elemental sulphur (S), and organic sulphur compounds such as mercaptans (RSH) rapidly attack copper, silver, aluminum, and

Table 3: Outdoor air pollutants and their sources.

Pollutants	Source	Influence
Sulphur dioxide(SO_2)/ Sulphur oxide(SO_X)	Burning coal and oil.	Forms acidic surface. Attack many meals.Stress corrosion accelerator
Nitrogen oxide(NO_X)/ Nitrogen dixide(NO_2)	Burning fuel in cars and other industrial processes.	Attack metals like Co, Ni, & Fe.Nitrate particles cause failures at microelectronic interface.
Carbon dioxide(CO_2)	Volcanic activity and hot springs, combustion processes, cars and power plants.	Inhibit the NaCl induced carbonate containing corrosion products of zinc and copper
Volatile organic compounds	Evaporates from sources such as vehicle exhausts, cleaning agents, and furniture polish and fabric softener.	Destabilizes passive film by lattice impregnation & acid dissolution.
Ammonia	Used to fertilise crops and emitted from this agricultural process and farm animals.	Complex with metal like Cu,Ni and Ag Forms basic surfaces
Persistent organic pollutants (POP)	Produced through industrial processes and waste incineration.	Corrosion of metal at even at low concentration.
Particulate matter (from sulphates and nitrates)	Fine particles which are either man made or natural.	Attack on metal like Co, Al increases with relative humidity.
Ozone	Formed from the chemical reaction during sunlights	Degrades polymers & accelerate oxidation of H_2S,NO_2 & SO_2

iron alloys at low concentration of ppb level. The presence of NO_2 with H_2S greatly enhances silver sulfidation in presence of high humidity content. Active sulphur compound with inorganic chlorides as predominant a constituents are the causes of corrosion in process industries. Failures in printed circuit boards, integrated circuits, and other components have been known to occur due to the atmospheric exposure even in extremely low levels of these gaseous contaminants. Cuprous oxide protects copper from further attack by sulphur compounds in a dry atmosphere. In humid condition, cuprous oxide present as an adsorbed film reacts with hydrogen sulphide to form $Cu_4SO_4(OH)_6.H_2O$ a corrosion products [104].

Sulphur dioxide:

Corrosion-induced failures are frequent in electronic products used in sulphur dioxide environments. Oxidation of sulphur dioxide forms sulphate ions in presence of moisture.

$$SO_2 + O_2 + 2e- \rightarrow SO_4^{2-} \quad (28)$$

The corrosion-stimulating sulphate ions are liberated during anodic dissolution leading to an auto-catalytic type of attack on the metal surface [105]. The acidification of the electrolyte also accelerates the corrosion rate, but this effect is likely to be of secondary importance because of the buffering effects of hydroxide and oxide corrosion products. At very high levels of sulphur dioxide, dissolution of protective layers and the formation of more soluble corrosion products are associated with higher corrosion rates. SO_2 pollutant substantially enhances the corrosion rates of metals exposed in the atmosphere. Rozenfeld [106] has suggested that, because of greater solubility (SO_2 is about 2600 times more soluble than oxygen); SO_2 might be reduced at cathodic sites more rapidly than oxygen, consequently increasing anodic dissolution rates. In solution, electro-chemical reduction of SO_2^{-3} competes with its oxidative conversion to SO_2^{-4}. However, Seinfeld, [107] states that, in the absence of catalysts, solution phase oxidation of SO_2^{-3} by dissolved oxygen is slow. Under these circumstances SO_2 may persist for a sufficient length of time to act as a cathodic depolarizer in the manner as suggested by Rozenfeld. Corrosion can occur quite rapidly in humid environments in presence of atmospheric sulphur and chlorides results intermittent equipment malfunctions, unplanned shutdowns, or failure of critical systems. A typical failure mechanism of electronic systems is the reaction of atmospheric sulphur with exposed metals – particularly copper and silver. These metals are found in PCB traces, integrated circuit (IC) leads and device terminations.

Silver creep corrosion (electromigration) readily occurs in humid environments in the presence of small amounts of sulphur and chloride. Sulphur-based corrosion failures increased dramatically upon introduction of immersion Ag surface finish on computer products (due to ROHS requirements). The majority of creep corrosion failures occurred on hard disk drives (HDD), graphic cards, and motherboards in desktop or workstation systems. Copper sulfide (Cu_2S) or silver corrosion products can grow and creep across surfaces such as IC packages and PCB substrates High amounts of Cu_2S typically indicate the presence of active sulphur compounds such as elemental sulphur (S), hydrogen sulphide (H_2S), or organic sulphur compounds such as mercaptans. Ag_2S can also be formed by these contaminants but can also be formed by exposure to sulphur oxide (SOx) contamination [108].

9.2 Nitrogen compounds

Nitrogen oxide compounds (NOx, NO_2, N_2O_4) have a major role in the formation of ozone in the atmosphere. Atmospheric oxidation of nitrous oxide to nitrogen dioxide and nitric acid takes place successfully with the following reaction,

$$2NO + O_2 \rightarrow 2NO_2 \quad (29)$$

$$2NO + H_2O + 3/2\ O_2 \rightarrow 2HNO_3 \quad (30)$$

The NO_2/NO ratio in the atmosphere varies with time and distance from the source. NOx may be further oxidized to form nitric acid. Eriksson and Johansson [109] exposed copper to humid air containing NO_2. Simon, et al., [110] studied the corrosion products formed on copper exposed to humid air containing NO_2 identified cuprite (Cu_2O) and basic copper nitrate($Cu_2(OH)_3NO_3$) on the surface usingXPS.The general conclusion of these studies is that NO_2 in the ppm range has very slight corrosive effects on copper.

9.3 Inorganic chlorine compounds

Inorganic chlorine compound includes chlorine (Cl_2), chlorine dioxide (ClO_4), hydrogen chloride (HCl); etc. and reactivity will depend upon the specific gas composition. Presence of Cl_2 in humid conditions, disintegrate into hypochlorite and chloride, hypochlorite is a strong oxidant, and chlorine has a strong synergetic effect with hydrogen

sulphide. Chloride has an ability to penetrate the oxides protecting metals and thus increases corrosion. Atmospheric salinity at low ppb react with metals like zinc, copper, tin, silver, and iron alloys accelerates corrosion. Feitnecht [111] carried out the major study of metals such as zinc, iron and copper which was exposed to HCl vapours at varying humidities between 50% and 95% RH, the value of which was approximately that of the vapor pressure over a saturated solution of the metal chloride formed during corrosion. The corrosion products found on zinc were $4Zn(OH)_2$. $ZnCl_2$, $Zn(OH)_2$ and ZnO.

9.4 Hydrogen peroxide

Hydrogen peroxide midsummer concentrations can be as high as 10-30 ppb and 10-100 µm precipitation often greater than those of SO_2 or SO_2^{-4} concentrations [112]. In recent years increased emissions of oxides of nitrogen and hydrocarbons have resulted in increase in atmospheric H_2O_2. The interactions of metal surface with H_2O_2 produces HO_X radicals.These oxidizing radiolytic products can have an inhibitive effect on the initiation of localized corrosion at potentials less than approximately +0.5 V vs. SHE, as are present in aqueous solutions exposed to the atmosphere [113].

9.5 Ozone

If the concentration of O_3 reaches to extreme values in urban areas, it can accelerate the sulphate and oxide formation in the atmosphere [114]. Later Graedel ET showed that O_3 enhances the atmospheric sulphidation of copper**.** Eriksson [115] found a basic copper sulphate, $Cu_2.5SO_4(OH)_3$. $2H_2O$, when exposed to SO_2+O_3 with 90% relative humidity. Ozone promotes the oxidation of SO_2 to sulphate more efficiently than NO_2. A synergism proposed between SO_2 and O_3 includes oxidation of Sulphur dioxide by ozone and the capability of ozone to form oxides, hydroxides or other oxygen containing reaction products in the presence of smaller amounts of SO_2. Presence of ozone may lead to an increase the deposition of sulphur dioxide on metals. Accelerating effect of ozone on zinc appears to be limited, but with aluminum and copper distinct corrosion degradation was observed. SO_2 induced atmospheric corrosion of copper increases the formation rate of both Cu_2O and $CuSO_4$. $x\,H_2O$ all over the surface [116,117,118].

9.6 Organic acids

Organic acids, such as acetic and formic acids, cause metal corrosion at very low concentrations. The presence of acetic acid and formic acids has been detected in the rain [119,120], where they increase the acidity. Acetic vapor from vinegar in the food processing industry also constitute about 0.1 to 1% of the total ion concentration in the copper exposed corrosion-products [119]

9.7 Saline particles

The amount of corrosion product formed increases with the amount of $(NH_4)_2SO_4$, particles, relative humidity (RH) and temperature [121,122,123]. At and above the critical relative humidity of $(NH_4)_2SO_4$, dissolution of Cu is followed by formation of Cu_2O, oxidation of Cu(I) ions to Cu(II) ions and precipitation of antlerite $[Cu_3(SO_4)(OH)_4]$, brochantite $[Cu_4(SO_4)(OH)_6]$, or posnjakite $[Cu_4(SO_4)(OH)_6.H_2O]$. Aluminum reacts with $(NH_4)_2SO_4$ particles only at or above the critical relative humidity (CRH) at either temperature. The corrosion rate increases with increasing RH and temperature [124].

10. Corrosion prevention techniques

There are several techniques to minimise corrosion and improve the conditions of protecting electronic devices.

10.1 Fault-resistant technique

Connectors, switches, relays and connections of other components and displays as well as the wiring pattern of the circuit board always affected with a risk of corrosion degradation. If the electrical/ mechanical functionality of the device requires very small tolerances in the signals, leakage currents or the size or quality of the impedances in the circuits (humidity affects the dielectric constant εr), the device will be sensitive to corrosion, since corrosion of the surfaces, contamination and humidity affect not only the metal surfaces but the electrical properties of the surfaces of the insulators as well. These changes in the serial resistances of the joints (connectors, solder joints, switches), leakage currents between the wires and insulation resistances caused by corrosion should be included in the sizing of the electric circuits in the designing of the device. Minimising the number of electromechanical connections, especially unprotected connections that can be opened, is a good means of reducing the corrosion risk.

10.2 Maintain dry atmosphere of the devices

A relatively tight device case is used to maintain the dry atmosphere in all situations since the presence of water always increases the risk for corrosion considerably and weakens the isolation of the surfaces.

Heat from the device itself should be used to minimise the harmful effects of humidity in order to keep the device dry and to ensure the removal of possible moisture inside the device. If the various parts of device kept warmer than its surroundings it would be easy to minimise the failure. The cooling air inside the device provides a natural help in the removal of moisture but if the flow is based only on weak natural convection or ventilation through cracks in the seals, precautions must be taken against long term effects of internal moisture and the inside surfaces must be better protected.

10.3 To use compatible material at joints

There are various boundary surfaces of materials on the circuit board, wiring patterns, connectors, switches and microcircuits etc. If the device is subjected to the corrosive substances present in air and to water galvanic corrosion occurs. High temperature and humidity accelerate these reactions. If same metal is used between the two surfaces then the smallest risk of corrosion occur. If the metals are different, the least corrosion occurs between surfaces where the electric surface potentials are as close to one another as possible. If the materials differ much in this respect, the probability for corrosion is great, if there is water and if there are corrosive gases in the air and on the surfaces. It is rather difficult in electronics devices to avoid contacts between different materials.These are naturally in contact with various metals. When using tin-lead solder, it should be checked that the circuit board or the component wires do not carry excessively thick layers of gold which forms intermetallic alloys with tin. The mechanical strength of these alloys is weak and they corrode quickly in heat.

10.4 Air filtration technique

If the outer and inner surfaces of electronic devices are in constant contact with gasous impurities and undesirable dust particles with faster air flow then the probability of chemical reactions (corrosion, humidification) and contamination is higher. The reduction of polluted airflow inside the device can prevent corrosion. The most common technologies available to deal with gaseous contaminations are (1) particle removal filtration such as mechanical filters and electronic air cleaners and (2) gas-phase (dry-scrubbing) filtration. Particulate filters vary in their ability to remove particulate matter, depending upon the filter's material composition (typically cellulose, fabric. and glass-fiber materials) and the efficiency of the filters is typically 20 to 65 percent [98,99,100]. Most instrumentation air conditioning systems come with low- to mid-efficiency filters already built into the system. Electronic air cleaners, another form of particulate filtration, use the principle of electrostatic precipitation. Particles are charged and then captured on collecting plates. They are relatively efficient against particles of sub-micron size, but require regular cleaning. Additionally, the electronic air cleaners produce ozone which may prove hazardous to human health, as well as causing corrosive damage to electronic circuitry if they are not installed and maintained properly.

Adsorption is the most common form of gas-phase filtration uses the processes of adsorption, and/or chemical reaction to remove gaseous contaminants from an airstream. The material most often used is carbon (activated and/or impregnated charcoal). Carbon is a very effective gas-filtration media due to its high porosity, large surface area presented to the airstream and high removal capacity. Gas-phase filtration systems typically have gas removal efficiencies of 99.95 percent. To reach this level of efficiency, a system may employ multiple media beds for taking advantage of the strengths of the media to target specific gases.Gas-phase air filtration technology has been used to protect crucial process control systems operating in harsh, industrial environments, is available for the protection of today's commercial data processing center. Gaseous contaminants, both externally and internally generated, can be effectively removed down to the low parts per billion levels to preclude any potential damage to electronic equipment.

11. Methods for testing devices due to corrosion

Corrosion tests are often accelerated tests. Humidity, elevated temperature and aggressive air born gaseous impurities are responsible accelerating factors to initiate corrosion. An examination of the combined effects of humidity, temperature and corroding gases by an accelerated test is a swift way of testing the durability of the circuit boards. The verification of the test conditions in the test chamber, the measurement of temperature and relative humidity, gas concentrations is a requirement for an accelerated test. The control of test conditions is limited by the analysing technique of gases. Various quick tests (shown in table 4) or more controlled standardised test gives fairly accurate information on the corrosion resistance properties of the products.

Table 4: Test employed to study corrosion degradation of electronic devices.

Test	Analysis
Failure Analyse Methods	Visual inspection photography, Microscopy,Measurement of resistance, Measurement of coatings, Material analysis, SEM
Rapid test methods	Water, humidity, salt solution, acid fume, Scraping, tape adhesion test, Chemicals, perfumes.
Heat tests Dry	Heat and cold (short and long period), Change of temperature, Combined cold/heat and cyclic humidity.
Humidity tests	Cyclic damp heat, Long period humidity at high temperature, Accelerated tests for components e. g. 85°C/85% RH
Gas tests	Multigas tests, H_2S, SO_2, NO_x , Cl^-, NH_4^+ etc
Salt mist tests Salt	Spraying salt solution mist
Tightness	Mechanical, dust and water tightness
Mechanical Tests	Vibration test, shock tests and fretting corrosion tests

This testing should be undertaken whenever the product is changed so that the changes may affect the tolerance for environmental conditions. When using new materials and components it should be checked that these actually function in the user conditions of the product.The testing and analysis methods listed in Table 4 are used for various coatings, component boards, components and entire devices. When the failure mechanisms are discovered it is possible to identify worthwhile corrective action for the next product generation [125].

12. Mixed Flowing Gas (MFG) Test

Mixed Flowing Gas (MFG) test is a method suitable for testing corrosion of electronic components caused by gaseous impurities in the air such as SO_2, H_2S, NO_2 and Cl_2. In flowing mixed gas test, a continuous flow of air including corrosive gases is directed through the test chamber and the various parameters such as temperature (^oC), relative humidity (%RH), concentration of gaseous pollutants (ppb level), and other critical variables (such as volume exchange rate and airflow rate) are carefully defined,monitored and controlled. In this way, the repeatability of the test conditions can be guaranteed. The consciously chosen humidity level, 70...85% RH is essential in these tests, as is the simultaneous use of two or more gases. This method produces tests revealing certain failure mechanisms fairly well and tests copying certain environmental conditions. Test samples that have been exposed to MFG testing have ranged from bare metal surfaces, to electrical connectors, and to complete assemblies. For noble metal plated connector applications, MFG test has been widely accepted as a qualification test method to evaluate the performance of these connectors.

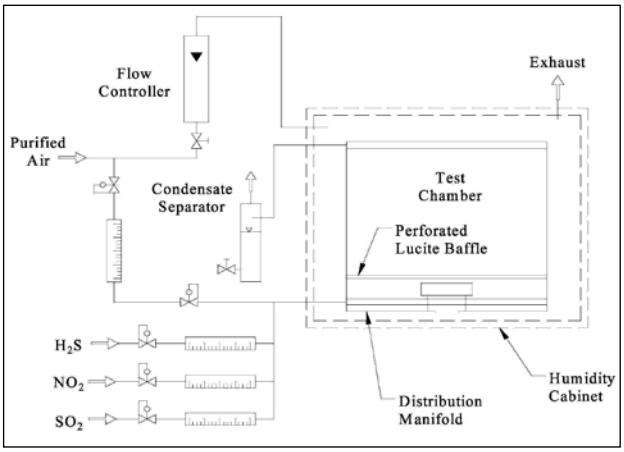

Fig.11: Mixed Flow Gas Test Chamber

The operational environments for electronic equipments in atmosphere are divided into four classes, from least corrosive (Class I) to most corrosive (Class IV). Class I means well-controlled office environment with continuous adjustment. Class II means light industrial environment, such as business offices without effective or continuous environment control. Class III means moderate industrial environment, such as storage areas with poor environment control. Class IV means heavy industrial environment, such as locations adjacent to primary sources of atmospheric pollutant gases. Since Class I indicate no precedent for environmental effects on reliability, there is no accelerated testing for Class I. The other three classes use a combination of corrosive gases such as NO_2, H_2S, Cl_2, and SO2 to accelerate corrosion [126,127]. Flowing mixed gas corrosion test, (H_2S + SO_2) method, the predominant fault mechanism is pore corrosion, so it is suited for pore corrosion testing of gold and palladium coatings copying mild indoor conditions. The creep of corrosion products can be detected with humidity and heat tests and mixed gas tests. (H_2S, NO_2, Cl_2) method, can be used for corrosion product creep tests since the

predominant fault mechanism in the test is the creep of corrosion products in addition to pore corrosion. These tests are also suitable for general reviewing of the corrosion sensitivity of the electronic components and simulating more demanding industrial conditions [125]. Since mixed flowing gas environment is an accelerated testing method, the determination of acceleration factor would be helpful to understand the reliability of the device [128].

13. Summary and Recommendations

This paper provides a comprehensive state of the art review of the corrosion induced degradation of electronic devices used in assembly processes. It also provides basic of atmospheric corrosion, influence of exposure parameters namely critical relative humidity, temperature, specific atmospheric corrodants (pollutants) and other atmospheric contaminant and airborne particles. It has been observed that more than 50% of microelectronic device failure is due to environmental conditions such as humidity or condensation, contaminants, ionic or organic residuals, temperature, thermal stress and electrical bias in various atmospheres such as rural, urban, industrial, marine, or combinations of these. The aim of the paper was to describe the corrosion induced degradation of device structure and methods of use on the corrosivity of the products for solving the corrosion problems so that designer can verify the correctness of the used corrosion protection technique and also find new approaches for product reliability. Therefore, corrosion control of electronic devices and know-how of various protection methods has become a major field of design in order to ensure product durability and competitiveness on a demanding market.

Corrosion essentially involves an electrochemical process and the driving force for this corrosion is the difference of electrochemical potentials between anode and cathode which may result from the dissimilar metals or alloys. Basic requirements for electrochemical corrosion includes the four condition such as (i) the metal anode, (ii) a cathode, (iii) electrolyte, usually condensate and salt or other contaminations, and (iv) a conductor to carry the flow of electrons from anode to cathode. The elimination of any one of the four conditions will stop corrosion. Because of wide temperature variations and high humidity, moisture tends to accelerate the corrosion and deterioration of the material can takes place. Under humid conditions serious problem such as fungus growth, changes in electrical characteristics and shortening can occur as a result of the accumulated moisture. Anodic, cathodic, and electrolytic reaction, uniform, galvanic, pitting and creep corrosion are the most common form of corrosion observed in electronics.

The most commonly used metals and alloys such as aluminium, gold, silver, tin, lead, nickel and their alloys will be corroded rapidely if subjected to condition of corrosive environment and high humidity. There are several factors that would accelerate the corrosion process, which needs to be controlled in order to reduce the corrosion effect in electronic system. In a practical working environment it is only possible to control corrosion by developing the quality system and proper planing. Many corrosion problems encountered could be avoided by proper design. Since corrosion as a phenomenon is always a complex combination of situations resulting from the environment, materials and the method of use of the device, advance measuring techniques are necessary to eliminate the corrosive effects of the environment and the sensitivity to corrosion of the device. Basic recommendation to minimize corrosion such as,

1. In order to minimise the corrosive effect it is necessary to use material for components, component boards and metal parts which can be compatible and relatively inert.
2. To use fault tolerant technology to ensures the operability of the production even though corrosion results in for example increased contact resistances and leakage currents. Use large tolerances of the components in the electric design and maximize the allowed changes of series resistances and leakage currents on the signal paths.
3. Minimize the air flow and its velocity inside electronics and use mechanical protecting covers; avoid bare meal surfaces in direct contact with each other to avoid bimetallic (galvanic) corrosion.
4. To avoid dissimilar metal couples, the tendency towards galvanic corrosion is greater between widely separated groups than between adjacent groups. Metals from different groups may be placed in contacts where suitable protection against galvanic action is provided through use of barrier tape protective coatings or other methods of isolation. Consider system compatibility environment, avoid the use of alloys susceptible to stress corrosion cracking.
5. Use corrosion resistant materials including plastics and nonmetallics in severe environments where possible. Galvanised support should be specified

during installation in neutral atmospheres and for inside installations where corrosive agents are present. Keep moisture away or provide for its removal.

6. Improve the environment by providing seals, dehumidification purges adequate ventilation, vapour phase inhibitors and air conditioning or by maintaining temperature above dew point. Protection of equipment against moisture, dust etc by use of storage in protected enclosure.

Corrosion control is of vital concern because corrosion of equipment and devices has a great effect on the operational and structural integrity of the system. A properly implemented corrosion programe will disclose corrosion attack in the early stages; minor maintenance can correct such corrosion. Preventive maintenance is the most cost effective method of controlling corrosion, including problem caused by poor design.

References

1. M.Datta, T.Osaka, J.W.Schultze. New trends in electrochemical technology .Microelectronic Packaging, 2005
2. Mark White, Joseph B. Bernstein. Physics-of-Failure Based Modeling and Lifetime Evaluation. Microelectronics Reliability, 2008, (5) 2/08.
3. Corrosion induced degradation of microelectronic http://www.tiscali.co.uk/reference/encyclopaedia
4. W. Tazibt, P. Mialhe, J.P. Charles, M.A. Belkhir. A junction characterization for microelectronic devices quality and reliability Microelectronics Reliability 2008,(48),348–353
5. Eijt Takeda, Kunihikeo, Ikuzaki et.el. VLSI Reliability Challenges:Device Physics to Wafer scale Systems.Micro elactron Reliability,1995,(35),325-363
6. DL Crook Evolution of VLSI Reliability Engineering .Pro. IRPS 1990 , 2-11
7. A.J. van Roosmalen and G.Q. Zhanga. Reliability challenges in the nanoelectronics era. Microelectronics Reliability 46 (2006),(46),1403-1414
8. B. Wunderle, B. Michel Progress in Reliability Research in the Micro and Nano Region, Microelectronics Reliability 2006,(46),1685–1694
9. H. Reichl, B. Michel, A. Schubert. Materials Science and Engineering – A MajorTopic in the Future of Micro-electronic Packaging. Proc. 3. Int. Conf. Micromaterials, April 2000, 72–73,
10. Microeletroics,http://www.microelectronics.com/stateofart
11. Articlesource:http://www.Intel/webpage
12. Dr. Alan Doolittle, Georgia Tech ECE 6450 -Source:http://www.google.com
13. Stamper AK, Fuselier MB, Tian X. Advanced wiring RC delay issues for sub-0.25-micron general CMOS. In Proceedings of Int. Interconnect Tech. Conf. (IITC), 1998, 62–68
14. Murarka SP. Low dielectric constant material for interlayer dielectric applications. Solid-StateTechnol 1996, (3),83–90
15. Martin P. Electronic failure analysis handbook. USA: McGraw-Hill; 1999.
16. Lau JH, Pao YH. Solder joint reliability of BGA, CSP, Flip Chip and fine pitch SMT assemblies. New York: McGraw-Hill; (1997).
17. Tsukada Y. New era of electronics packaging and its technical difficulties. In: Proceedings of ASME Advances in Electronic Packaging, 1999, 1-4.
18. Blackwell GR. Direct chip attach. Electronic packaging handbook. Boca Raton (FL): CRC Press; 1999.
19. Clech J-P. Lead-free soldering, pb-free solder joint reliability .Springer Publications; 2006,145-172
20. Dasgupta A, Pecht M. Material failure mechanisms and damage models. IEEE Trans Reliability;1991, 40(5), 531–536
21. Lall P. Tutorial.Temperature as an input to microelectronics – reliability models. IEEE Trans Reliability,1996 45(1),3–9
22. Semiconductor devices-mechanical and climatic test methods-Parts 25. Temp Cycling. 2003; IEC 60749-25 ED. 1.0 B
23. Semiconductor devices-mechanical and climatic test methods-Parts 34: Power cycling. 2005;IEC 60749-34 Ed. 1.0 B
24. J. A. Mclinn. Constant failure rate—a paradigm in transition. Quality and Reliability Engineering International, 1990, (6), 237–241.
25. J. B. Bowles. A survey of reliability-prediction procedures for microelectronic devices. IEEE Transactions on Reliability, March 1992, (41), 2–12.
26. W. Denson.The history of reliability prediction IEEE Transactions on Reliability.1998 (47)321–328.
27. Bowels JB. A survey of Reliability–Prediction Procedures for microelectronic devices. IEEE Trans Reliability 1992, (41), 2-12
28. Cushing M.J.,Mortin DE,Stadterman TJ,Malhotra A. Comparision of Electronic Reliability assesment approach .IEEE Trans Reliabilty, 199, (42), 542-543
29. Chang Raymond.Physical Chemistry for Boiscience USA University Science Book 2005,338-342
30. M. G. Pecht, F. R. Nash. Predicting the reliability of electronic equipment.Proceedings of the IEEE, 1994 (82), 992–1004.
31. E. Suhir, R.C.Cammarata, D.D.L.Chung, M.Jono."Mechanical Behavior of Materials and Structures in Microelectronics", Materials Research Society Symposia Proceedings, 1991, (226)
32. Tu RH, Rosenbaum E, Chan WY, Li CC, Minami E, Quader K Berkeley. Reliability Tools-BERT. IEEE Trans Computer-aided Des Integrated Circuits Syst; 1993, (12), 1524–34
33. Electronic Materials Handbook. ASM international 1989, (1), 1-1140.
34. Ying Zheng. Study of Copper Applications and Effects of Copper Oxidation in Microelectronic Package, May 10, 2003.
35. W.A. Lanford, P.J. Ding, W. Wang, S. Hymes, S.P. Murarka. "Alloying of copper for use in microelectronic metallization," .Materials Chemistry and Physics, 1995, (41), 192-198.
36. J.R. Lloyd, Mat. Res. Soc. Symp. Proc. 1992, (239), 667-676

37. C. Kittel. Introduction to Solid State Physics.7th edition, 1996, 160.
38. ASM handbook, Corrosion, 9th ed. ASM international 1987,(13), 610-640
39. Z.E Horvath, G. Peto, Z.Paszti, E. Zsoldos, E. Szilagyi, G. Battistig. Enhancement of oxidation resistance in Cu and Cu (Al) thin layer . Nuclear Instruments and Methods in Physics Research 1999 B 148
40. C.W. Tan, A.R. Daud, and M.A. Yarmo.Corrosion Study at Cu-Al Interface in Microelectronics Packaging .Applied Surface Science 2002,191.
41. G.L. Ang, L.C. Goh, K.W. Heng, S.K. Lahiri.Oxidation of Copper Lead Frame. International Symposium on the Physical & Failure Analysis of Integrated Circuits, 1995.
42. O. Yoshioka, O. Okabe, R. Yamagishi, S. Nagayama, G. Murakami.Improvement of moisture in plastic encapsulants MOS-IC by surface finishing copper lead fame. Proceedings-Electron Components Conference, 1989, 464-471.
43. source: www.synl.ac.cn/org/mic/english/index.htm
44. Robert S. Mroczkowski.Connector Design/Materials and Connector Reliability. AMP Incorporated, 1993.
45. J.A.Abys, Y.Okinaka, G.J.Russ, B.T.Kerns. Connectors, 35th Meeting of International Society of Electrochemistry, Berkeley, CA, 1984.
46. J.A.Abys. Connectors `87. Institute of metal Finishing, Coventry, England, 1987.
47. J.A.Abys, J.J.maisano, C.Wolowodiuk and H.K.Straschil, Connectors `89, Institute of Metal finishing, Coventry, England 1989.
48. A.Abys, G.F.Breck, H.K. Straschil, I.Boguslavasky, G.Holmbom, Palladium and Gold plating in connectors Plating Surf. Finish, 1998 86(1), 108.
49. H.H. Manko. Solder and Soldering, 2nd Edition, McGraw-Hill, New York,1979,151-159
50. R.E. Reed-Hill.Physical Metallurgy Principles, PWS Publishing Company, Massachusetts,1994,306-307
51. W.F. Smith. Principles of Materials Science and Engineering, 2nd Edition, McGraw-Hill, New York, 1990, 724.
52. M. Abtew. Corrosion of Solders Induced by Flux Residue and Ionic Contamination, Amdahl Corporation, Technical Bulletin, 1993.
53. J.H. Vincent, B.P. Richards. Alternative solders for electronics assemblies . Circuit World 1993, 19 (3), 33.
54. Casas, Jose S.; Sordo, Jose, eds. Lead Chemistry, Analytical Aspects. Environmental Impacts and Health Effects.2006
55. Xuan X, Chatterjee A, Singh AD, Kim NP, Chisa MT. IC reliability simulator ARET and its application in design-for-reliability, In: Proceedings of the 12th Asian test symposium, 2003, 19-22.
56. Yoram Shapira, Michael Talmor. Electronic circuit reliability modelling Joseph B. Bernstein, 1957–1979, Microelectronics Reliability 2006, (46) ,957-979.
57. M. Yunovich, Electronics, Appendix Z-ppZ1-Z72. articlesource-www.corrosioncost.com/pdf/electronic.pdf,
58. McPherson. Corrosion and Reliability of Electronic Materials and Devices, Electrochem. Soc., 1994 (27), 29-50.
59. Comizzoli R B, Frankenthal R P, Milner P C.Corrosion of electronic materials and devices.1986, *Science* -340,
60. John W. Osenbach.Corrosion induced degradation of microelectronic devices, semicond.sci. Technol. 1996,(11),155-162
61. Iannuzzi M. Development and evolution of a pre-encapsulation cleaning process to improve reliability of HIC's with aluminium metallized chips. Reliability Physics 1981, (19), 228
62. Iannuzzi M. Bias humidity performance and failure mechanisms of non-hermetic SIC's in an environment contaminated with Cl2, IEEE Trans. Components Hybrids Manuf. Technol.1983,(2**),** 191.
63. Paulson W M,Lorigan R P, The effect of impurities on corrosion of aluminium metallization 14th Ann. Proc. Reliability Phys. (New York: IEEE) 1986, (44) ,112.
64. Andrew H. Rawwicz. Stress induced corrosion of wire micro-joints in microelectronics – a quantitative model. Microelectronics and Reliability, 1994, 34(5) 875-882.
65. Bagdonavicius, Vilijandas; Nikulin, Mikhail. Accelerated Life Models. Modeling and Statistical Analysis, Chapman&Hall/CRC,2002
66. F.P. Mc. Pecht M. A corrosion rate equation for microelectronic die metallization International Journal of Hybrid Microelectronics 1990, 13(2), 41-52.
67. F.P. Mc Cluskeya, Y.D. Kweona. Method for assessing remaining life in electronic assemblies. Microelectronics Reliability 2000, (40), 293-306
68. Fu-gin Chen and A. Jean Osteraas. Electrochemical dendrite formation duringcorrosion of connector leads. Proceedings of ASM's third conference on electronic packaging: materials and processes and corrosion in microelectronics.1987, 175-179.
69. Osenbach J W. Water-induced corrosion of materials used for semiconductor passivation. Electrochemical Society 1993, (40), 36-67.
70. Pecht M. A model for moisture induced corrosion failures in microelectronic packages. IEEE transactions on components hybrids and manufacturing technology,1990, 13(2), 383-389
71. Stroehle D, on the penetration of gases and water vapour. New York: IEEE, Int. Reliability Physics Symp.1977, 101.
72. Schnable G L, Comizzoli B L, Kern W, White L K. A survey of corrosion failure mechanisms in microelectronic devices. *RCA Rev.1979, (*40)**,** 416.
73. Krumbein, S.J. Tutorial: Electrolytic models for metallic electromigration failure mechanisms. IEEE Transactions on Reliability, 1995, (44), 539–549.
74. Katayanagi, H., Tanaka, H., Aoki Y., Yamamoto, S.The effects of adsorbed water on printed circuit boards and the process of ionic migration,ESPEC Technology Report, 2000, (9) ,15–20
75. Chazalviel, J.N.Electrochemical aspects of the generation of ramified metallic electrodeposits. Physical Review *A*, 1990, (42), 7355–7367.
76. Fleury, V., Rosso, M., Chazalviel J.N. Geometrical aspect of electrodeposition: the Hecker effect. Physical Review 1991, (43), 6908–6916.
77. Welsher, T.L., Mitchell, J.P., Lando, D.J. CAF in composite printed circuit substrates: characterization, modeling and a resistant material, IEEE Proceedings of International Reliability Physics Symposium,1980, 235-237
78. Reid, M., Punch, J., Rodgers, B., Pomeroy, M.J., Galkin. Factors that influence ionic migration on printed wiring boards. IEEE Proceedings of International Reliability Physics Symposium. 2005, 300-304.

79. X.J. Fan, E. Suhir (Eds.). Moisture Sensitivity of Plastic Packages of IC Devices. Micro- and Opto-Electronic Materials, Structures, and Systems, Springer Science+Business Media, LLC, 2010.
80. Harsanyi, G. Irregular effect of chloride impurities on migration failure reliability: contradictions or understandable Microelectronics Reliability, 1999, (39), 1407–1411
81. Nieman, D.A. Effect of contamination on copper migration in TAB tape structures. IEEE International Reliability Physics Symposium, 1994, 87-92.
82. Apicella, A., R., De Cataldis, C. Sorption modes of water in glassy epoxies. Journal of Membrane Science, 1984 (18), 211–225.
83. Luo, S., Wong, C.P., Leisen, J. Fundamental study on moisture absorption in epoxy for electronic applications. International Symposium on Advanced Packaging Materials, 2001, 293–298.
84. whisker, Articlesource "http://nepp.nasa.gov/WHISKER/background/index.htm
85. C. L. Rodekohr, G. T. Flowers. Influence of Quantifiable Extrinsic Stresses on Tin Whisker Growth ASME, 2009.
86. C. L. Rodekohr, G. T. Flowers, Measurements on High Aspect Ratio Sn Whiskers, Proc. 54th IEEE Holm Conference on Electrical Contacts, October 2008, 231-234.
87. Qian Sun, Understanding and Minimization of Tin Whiskers Course, Spring 2003. MatE 234 800-14-0839
88. B.-Z. Lee, D.N. Lee, Spontaneous growth mechanism of tin whiskers .Acta mater, 1998, (46), 3701-3714.
89. Chen Xu, Chonglun Fan, and Joseph A. Abys, Whisker prevention, APEX, proceedings of the technical conference, 2003.
90. John O'Boyle.Tin Whiskers Are Real and Complex Maxim Integrated Products, Inc.Dec,13,2011
91. Chen Xu, Yun zhang, Chonglun Fan, and Joseph A. Abys. Understanding whisker phenomenon-driving force for the whisker formation. APEX,proceedings of the technical conference, Jan 2002, S 06-1-1,
92. M. Endo, S. Higuchi, Y. Tokuda, Y. Sakabe. Elimination of whisker growth on tin plated electrodes. International Symposium for Testing and Failure Analysis proceedings, Oct 1997, 305-311.
93. B. D. Dunn. A laboratory study of tin whisker growth, 1987, ISSN 0379 4067.
94. Jong S. Kadesch ,Jay Brusse.The continuing dangers of tin whiskers and attempts to control them with conformal coating," Tinwhisker Articlesource: www.google.com
95. Kathleen M. Cunningham, Michael P. Donahue, Tin whiskers: mechanism of growth and prevention, 4th International SAMPE Electronics Conference, June 1990.
96. Rob Schetty. Minimization of tin whisker formation for lead-free electronics finishing, IPC Works Conference Proceeding, Mami, 2000.
97. Naixin X, Zhao L, Ding C, Zhang C, Li R ,Zhong Q. Atmospheric Corrosion . Corros. Sci. 2002 (44), 163.
98. Brown P.W, Masters L.W. Atmospheric Corrosion, Wiley, New York, 1982.
99. Standard: ANSI/ISA S71.04-1985, Environmental Conditions for Process Measurement and Control Systems: Airborne Contaminants, Instrument Society of America, Research Triangle Park, NC, (1985).
100. Boonzaier, W.G. Acid Gas Corrosion Protection. SA Measurement & Control, July, 1986, 5-9.
101. Naeemi A.H, Albrecht P. Int. Cong.Metallic Corros. Toronto, Canada, 1984, 418.
102. Money K. L. Metals Handbook Corrosion, ASM International, 1987, 204.
103. Vilche J. R, Varela F.E, Acuna G, Codaro E.N, Rosales B.M, Fernandez A . Corros. Sci., 1995, (37), 941.
104. Abbott W.H, Proc. 16th Int. Conf, Electrical Contacts, Loughborough, England, 1992.
105. Barton K, Protection against Atmospheric Corrosion, John Wiley and Sons, London, 1976.
106. Rozenfeld I.L, Proc. 1st Int. Cong. Metallic Corros. Butterworth, London, 1961, 243.
107. Seinfeld J.H, the Atmospheric Chemistry and Physics of Air Pollution, Wiley, New York. 1986.
108. Memphis S. Proceedings of TAPPI Engineering, Pulping, Environmental Conference: Innovations in Energy, Fiber and Compliance 2009.
109. Ericsson P and Johansson L.G, Proc. 1^{0th} Scandinavian Corros. Cong., Stockholm. 1986.
110. Simon D, Mollimard D, Perrin C ,Bardolle J, Proc. 14th Int. Conf. Electric Contacts, Paris ,1988.
111. Barton K and Bartonova Z, Proc. 3rd Int.Congr. Metallic Corros. 1969, (40), 403.
112. Graedel T.E, Electrochem. Soc., 1986, (133), 2476.
113. Garrels R.M, Geochim. Cosmochim. Acta, 1954, (5), 153.
114. Tidblad J, Leygraf C. Electrochem.Soc.1995, (142), 749.
115. Eriksson P, PhD Thesis. Chalmers University of Technology, Goteborg, Sweden. 1992.
116. Zakipour S, Tidblad J, Leygraf C.Electrochem. Soc.1995, (142), 757.
117. Oesch S, Faller M.Corros. Sci.1997, (39), 1505.
118. Aastrup T, Wadsak M, Schreiner M and Leygraf C. Electrochem. Soc.2000, (147), 2543.
119. Galloway J.N, Likens G.E, Water Air Soil Poll.1976 (6), 241.
120. Graedel T.E, McGrory-Joy C, Franey J.P. Electrochem. Soc.1986 (133), 452.
121. Lobnig R.E, Frankenthal R.P, Siconolfi D, J, Sinclair J.D. Electrochem. Soc. 1993, (140), 1902.
122. Sinclair J.D, Psota-Kelty L.A Atmos.Environ. 1990 (24A), 627.
123. Lobnig, R.E., Frankenthal R.P, Siconolfi J.D, Sinclair J.D, Stratmann M .Electrochem. Soc.1994 (141), 2935.
124. Lobnig, R.E, Siconolfi D.J, Maisano J, GrundmeierG, Streckel H, Sinclair J.D, Electrochem. Soc.1996 (143), 1175.
125. Risto Hienonen & Reima Lahtinen, Corrosion and climatic effects in electronics VTT PUBLICATIONS 626 .ESPOO 2007.
126. American Society for Testing and Material, ASTM Designation B845-97: Standard Guide for Mixed Flowing Gas (MFG) Tests for Electrical Contacts, 1997.
127. Gore, R.R., Witska, R., Kirby, J.R. Chao, J.L.Corrosive Gas Environmental Testing for Electrical Contacts. IEEE Transactions on Components, Packaging, and Manufacturing Technology, March 1990(13/1), 27-32.
128. Williams, D.W.The Effect of Test Environment on the Creep of Base Metal Surface Films over Precious Metal Inlays.IEEE Transactions on Components, Hybrids and Manufacturing Technology, 1988, (11), 36-42.

SRESA JOURNAL SUBSCRIPTION FORM

Subscriber Information (Individual)

Title	First Name	Middle Name	Last Name
_____	_____	_____	_____

Street Address Line 1	Street Address line 2		
_____	_____	_____	_____
City	State/Province	Postal Code	Country

Work Phone	Home Phone	E-mail address
_____	_____	_____

Subscriber Information (Institution)

Name of Institution/ Library _____

Name and Designation of Authority for Correspondence _____

Address of the Institution/Library _____

Subscription Rates

	Subscription Quantity	Rate	Total
Annual Subscription (in India)	_____	Rs. 15, 000	_____
(Abroad)	_____	$ 500	_____
	_____		_____
	_____		_____

Payment mode (please mark)

Cheque ☐ Credit Card ☐ Master Card ☐ Visa ☐ Online Banking ☐ Cash ☐ De mand Draft ☐

Credit card Number _____

Credit Card Holders Name _____

Credit Card Holde _____

Guidelines for Preparing the Manuscript

A softcopy of the complete manuscript should be sent to the Chief-Editors by email at the address: editor@sresa.org.in. The manuscript should be prepared using 'Times New Roman' 12 font size in double spacing, on an A-4 size paper. The illustrations and tables should not be embedded in the text. Only the location of the illustrations and tables should be indicated in the text by giving the illustration / table number and caption.

The broad structure of the paper should be as follows: a) Title of the paper – preferably crisp and such that it can be accommodated in one or maximum two lines with font size of 14 b) Name and affiliation of the author(s), an abstract of the paper in ~ 100 words giving brief overview of the paper and d) Five key words which indicates broad subject category of the paper. The second page of the paper should start with the title followed by the Introduction

A complete postal address should be given for all the authors along with their email addresses. By default the first author will be assumed to be the corresponding author. However, if the first author is not the corresponding author it will be indicated specifically by putting a star superscript at the end of surname of the author.

The authors should note that the final manuscript will be having double column formatting, hence, the size of the illustration, mathematical equations and figures should be prepared accordingly.

All the figures and tables should be supplied in separate files along with the manuscript giving the figure / table captions. The figure and table should be legible and should have minimum formatting. The text used in the figures and tables should be such that after 30% reduction also it should be legible and should not reduced to less than font 9.

Last section of the paper should be on list of references. The reference should be quoted in the text using square bracket like '[1]' in a chronological order. The reference style should be as follow:

1. Pecht M., Das D, and Varde P.V., "Physics-of-Failure Method for Reliability Prediction of Electronic Components", Reliability Engineering and System Safety, Vol 35, No. 2, pp. 232- 234, 2011.

After submitting the manuscript, it is expected that reviews will take about three months; hence, no communication is necessary to check the status of the manuscript during this period. Once, the review work is completed, comments, will be communicated to the author.

After receipt of the revised manuscript the author will be communicated of the final decision regarding final acceptance. For the accepted manuscript the author will be required to fill the copy right form. The copy right form and other support documents can be down loaded from the SRESA website: http://www.sresa.org.in

Authors interested in submitting the manuscript for publication in the journal may send their manuscripts to the following address:

Society for Reliability and Safety
RN 68, Dhruva Complex
Bhabha Atomic Research Centre,
Mumbai – 400 085 (India)
e-mail : editor@sresa.org.in

The Journal is published on quarterly basis, i.e. Four Issues per annum. Annual Institutional Subscription Rate for SAARC countries is Indian Rupees Ten Thousand (Rs. 10,000/-) inclusive of all taxes. Price includes postage and insurance and subject to change without notice. For All other countries the annual subscription rate is US dollar 500 ($500). This includes all taxes, insurance and postage.

Subscription Request can be sent to SRESA Secretariat (please visit the SRESA website for details)

SRESA's International Journal of

Life Cycle Reliability and Safety Engineering

Contents

Vol.3 Issue No.4 Oct-Dec 2014 ISSN – 2250 0820